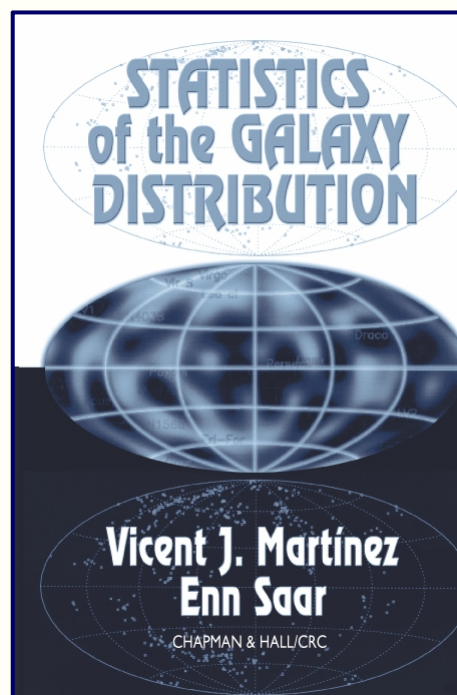


Measures of Cosmic Structure

Lecture course LSS2012
University Groningen
Nov. 2012-Jan 2013

Standard to
Reference:

Martinez & Saar



Ergodic Theorem

Statistical Cosmological Principle

Cosmological Principle:

Universe is Isotropic and Homogeneous

Homogeneous & Isotropic Random Field $\psi(\vec{x})$:

Homogenous	$p[\psi(\vec{x} + \vec{a})] = p[\psi(\vec{x})]$
Isotropic	$p[\psi(\vec{x} - \vec{y})] = p[\psi(\vec{x} - \vec{y})]$

Within Universe one particular realization $\psi(\vec{x})$:

Observations: only spatial distribution in that one particular $\psi(\vec{x})$
Theory: $p[\psi(x)]$

Ergodic Theorem

Ensemble Averages \longleftrightarrow Spatial Averages
over one realization
of random field

- Basis for statistical analysis cosmological large scale structure
- In statistical mechanics Ergodic Hypothesis usually refers to time evolution of system, in cosmological applications to spatial distribution at one fixed time

Ergodic Theorem

Validity Ergodic Theorem:

- Proven for Gaussian random fields with continuous power spectrum
- Requirement:

spatial correlations decay sufficiently rapidly with separation

such that

many statistically independent volumes in one realization



All information present in complete distribution function $p[\psi(\vec{x})]$ available from single sample $\psi(x)$ over all space

Fair Sample Hypothesis

- Statistical Cosmological Principle
- +
- Weak cosmological principle
(small fluctuations initially and today over Hubble scale)
- +
- Ergodic Hypothesis

fair sample hypothesis
(Peebles 1980)

Discrete e.g. Continuous

Discrete & Continuous Distributions

- How to relate discrete and continuous distributions:
- Define number density $n(\vec{x})$ for a point process:

$$n(\vec{x}) = \bar{n}[1 + \delta(\vec{x})] = \sum_i \delta_D(\vec{x} - \vec{x}_i)$$

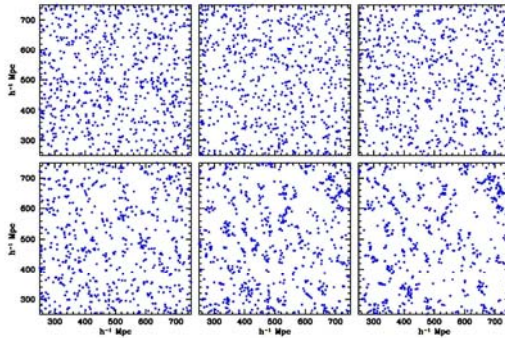
$\delta_D(\vec{x})$

Dirac Delta function

$$\left\langle \sum_i \delta_D(\vec{x} - \vec{x}_i) \right\rangle = \bar{n} \quad \text{ensemble average}$$

Correlation Functions

Correlation Functions

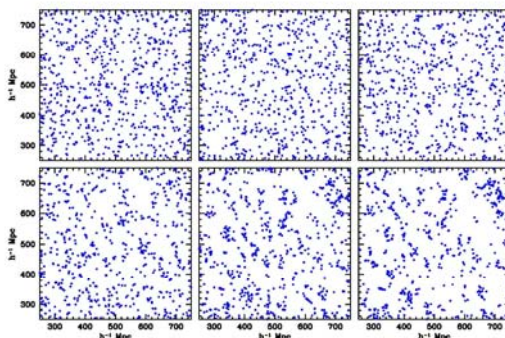


Joint probability that
in each one of
the two infinitesimal volumes
 dV_1 & dV_2 ,
at distance r ,
lies a galaxy

Infinitesimal Definition Two-Point Correlation Function:

$$dP(r) = \bar{n}^2 (1 + \xi(r)) dV_1 dV_2$$

Correlation Functions



In case of
Homogeneous & Isotropic
point process

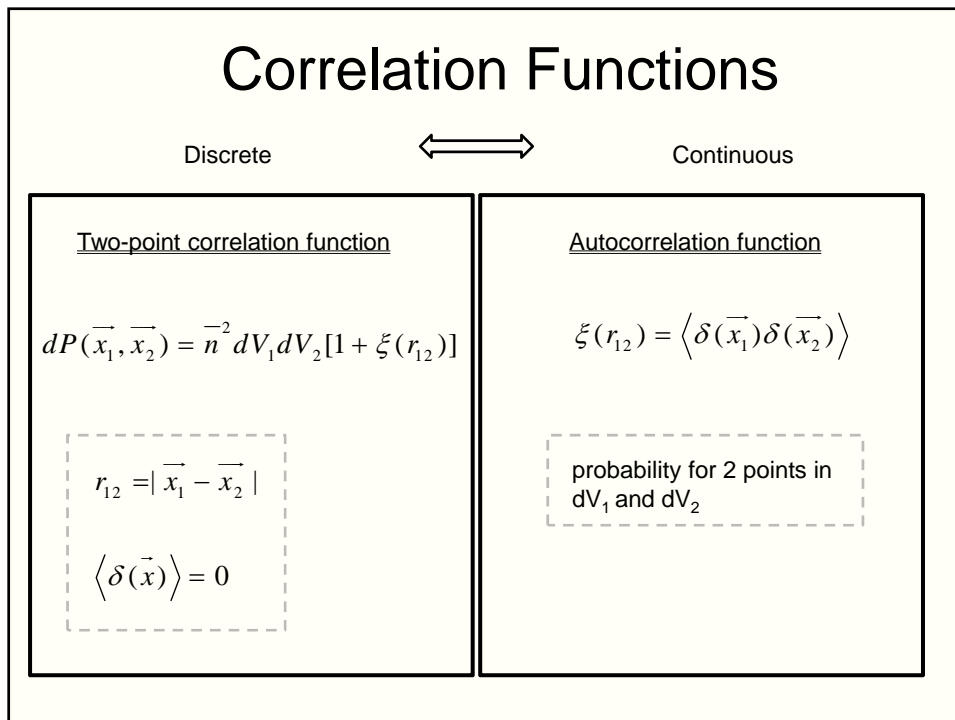
then $\xi(\vec{r})$

only dependent on

$$|\vec{r}| = r$$

Infinitesimal Definition Two-Point Correlation Function:

$$dP(r) = \bar{n}^2 (1 + \xi(r)) dV_1 dV_2$$



Correlation Functions

- Gaussian (primordial and large-scale) density field:
 - Autocorrelation function $\xi(r)$ Fourier transform power spectrum $P(k)$
 - $$\xi(\mathbf{r}) = \xi(|\mathbf{r}|) = \int \frac{d\mathbf{k}}{(2\pi)^3} P_f(k) e^{-i\mathbf{k}\cdot\mathbf{r}}$$
 - Autocorrelation function completely specifies statistical properties of field
- First order measure of deviations from uniformity
- Nonlinear objects (halos):
 - $\xi(r)$ measure of density profile
- Large Scales:
 - related to dynamics of structure formation via e.g. cosmic virial theorem

Correlation Functions: related measures

Other measures related to $\xi(r)$:

- Second-order intensity $\lambda_2(r) = \bar{n}^2 \xi(r) + 1$
- Pair correlation function $g(r) = 1 + \xi(r)$
- Conditional density $\Gamma(r) = \bar{n}(1 + \xi(r))$

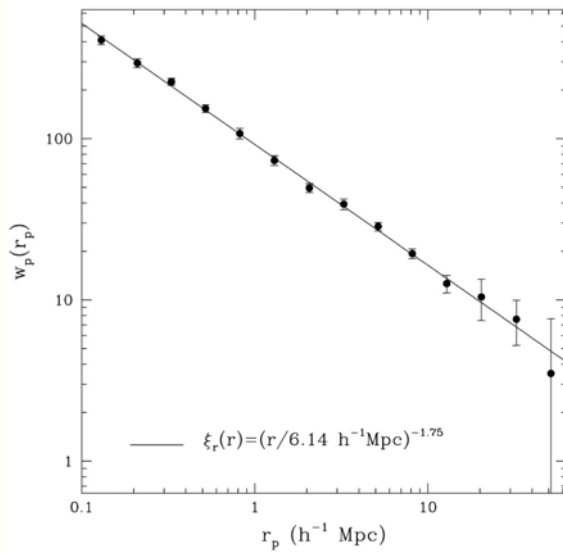
Correlation Functions: related measures

$$J_3(r) \equiv \int_0^\infty \xi(y) y^2 dy$$

Volume averaged correlation function $\bar{\xi}(r)$

$$\bar{\xi}(r) = \frac{3}{4\pi r^3} \int_0^r 4\pi \xi(x) x^2 dx = \frac{3J_3(r)}{r^3}$$

Power-law Correlations



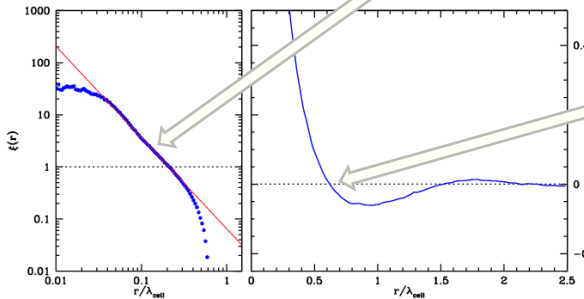
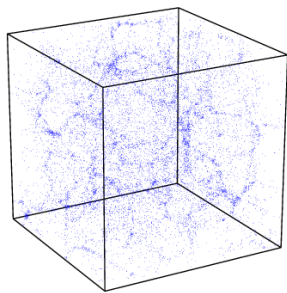
$$\xi(r) = \left(\frac{r}{r_0}\right)^{-\gamma}$$

$$\gamma \approx 1.8$$

$$r_0 \approx 5 h^{-1} \text{Mpc}$$

Totsuji & Kihara 1969
 Peebles 1975, 1980, ...

Correlation Functions



$$\xi_{cc}(r) = \left(\frac{r_0}{r}\right)^\gamma$$

$$\xi(r_0) = 1$$

Clustering length/
 "Correlation" length

Coherence length

$$\xi(r_a) = 0$$

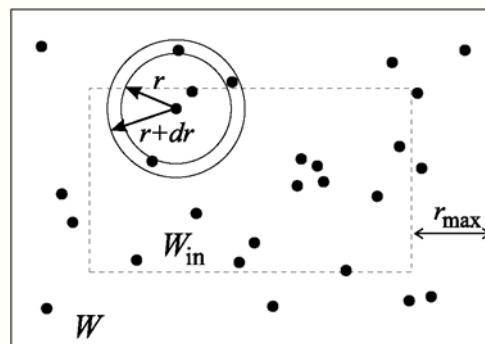
Correlation Function Estimators

Minimal Estimator

$$\hat{\xi}_{\min}(r) = \frac{V(W)}{NN_{in}} \sum_{i=1}^{N_{in}} \frac{n_i(r)}{V_{sh}} - 1$$

For galaxies close to the boundary the number of neighbours is underestimated. One way to overcome this problem is to consider as centers for counting neighbours only galaxies lying within an inner window W_{in}

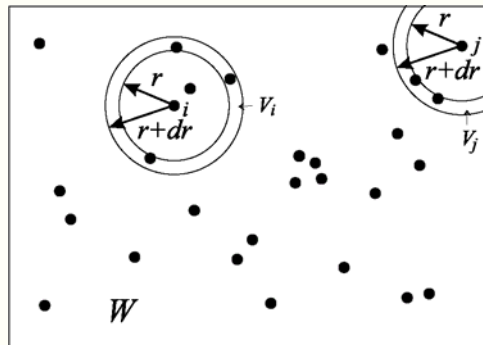
V_{sh} is the volume of the shell of width dr



Edge-Corrected Estimator

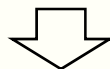
$$\hat{\xi}_{edge}(r) = \frac{V(W)}{N^2} \sum_{i=1}^{N_{in}} \frac{n_i(r)}{V_i} - 1$$

- $N_i(r)$: number of neighbours at distance in the interval $[r, r+dr]$ from galaxy i
- V_i : volume of the intersection of the shell with W
- W : when W a cube, an analytic expression for V_i can be found in Baddely et al. (1993).



Estimators Redshift Surveys

- In redshift surveys, galaxies are not sampled uniformly over the survey volume
- Depth selection:
in magnitude-limited surveys, the sampling density decreases as function of distance
- Survey Geometry
boundaries of survey often nontrivially defined:
 - slice surveys
 - non-uniform sky coverage
 - etc.



Clustering in survey compared with sample of Poisson distributed points, following the same sampling behaviour in depth and survey geometry

Difference in clustering between
data sample (D) and Poisson sample (R)
genuine clustering

Estimators Redshift Surveys

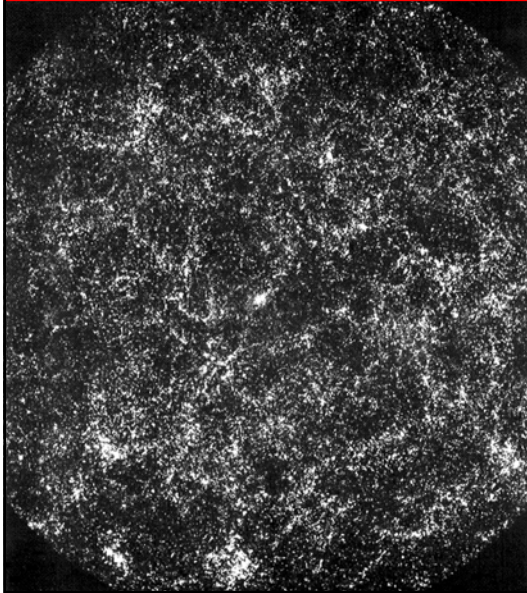
Clustering in survey compared with sample of Poisson distributed points, following the same sampling behaviour in depth and survey geometry

Difference in clustering between
data sample (D) and Poisson sample (R)
genuine clustering

- $\xi_{DP}(r) = \frac{n_R}{n_D} \frac{\langle DD \rangle}{\langle RR \rangle} - 1$ Davis-Peebles
(1983)
- $\xi_{Ham}(r) = \frac{\langle DD \rangle \langle RR \rangle}{\langle DR \rangle^2} - 1$ Hamilton
(1993)
- $\xi_{LS}(r) = 1 + \left(\frac{n_R}{n_D} \right)^2 \frac{\langle DD \rangle}{\langle RR \rangle} - 2 \frac{n_R}{n_D} \frac{\langle DR \rangle}{\langle RR \rangle}$ Landy-Szalay
(1993)

Angular
Two-point Correlation Function

Angular Correlation Function



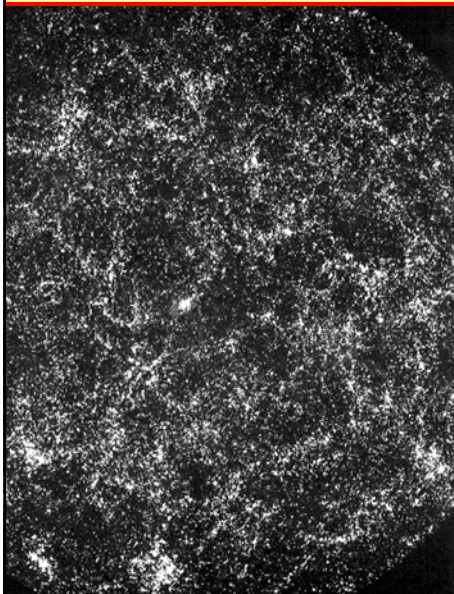
Galaxy sky distribution:

- Galaxies clustered, a projected expression of the true 3-D clustering
- Probability to find a galaxy near another galaxy higher than average (Poisson) probability
- Quantitatively expressed by 2-pt correlation function $w(\theta)$:

$$dP(\theta) = \bar{n}^2 \{1 + w(\theta)\} d\Omega_1 d\Omega_2$$

Excess probability of finding 2 gal's at angular distance θ

Angular & Spatial Clustering



$$dP(\theta) = \bar{n}^2 \{1 + w(\theta)\} d\Omega_1 d\Omega_2$$



Two-point angular correlation function is the "projection" of $\xi(r)$

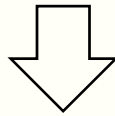
Limber's Equation:

$$w(\theta) = \frac{\iint p(\bar{x}_1) p(\bar{x}_2) x_1^2 x_2^2 dx_1 dx_2 \xi(|\bar{x}_1 - \bar{x}_2|)}{\left[\int_0^\infty x^2 p(x) dx \right]^2}$$

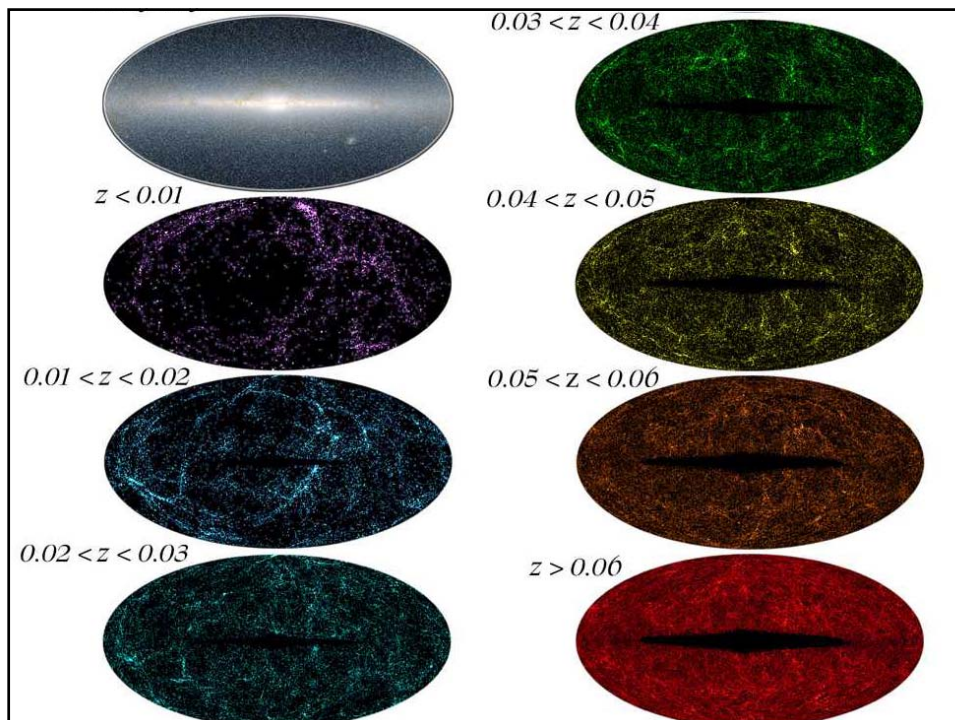
$p(x)$: survey selection function

Limber Equation

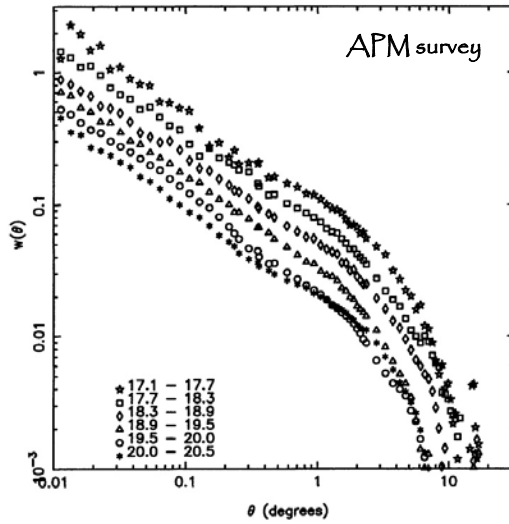
$$w(\theta) = \frac{\iint p(\vec{x}_1) p(\vec{x}_2) x_1^2 x_2^2 dx_1 dx_2 \xi(|\vec{x}_1 - \vec{x}_2|)}{\left[\int_0^\infty x^2 p(x) dx \right]^2}$$



$$\xi(r) = \left(\frac{r_0}{r} \right)^\gamma \longleftrightarrow w(\theta) = A \left(\frac{1}{\theta} \right)^{\gamma-1}$$



Angular Clustering Scaling



Two-point correlation function:

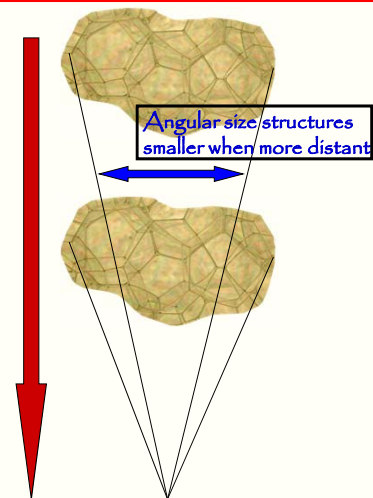
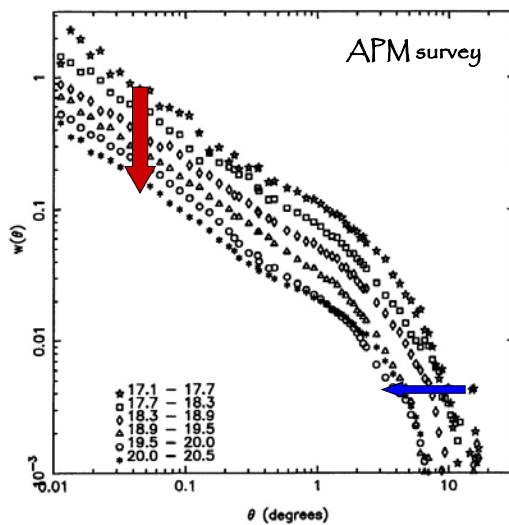
- small angles: power-law

$$w(\theta) = \left(\frac{\theta_0}{\theta} \right)^\gamma$$

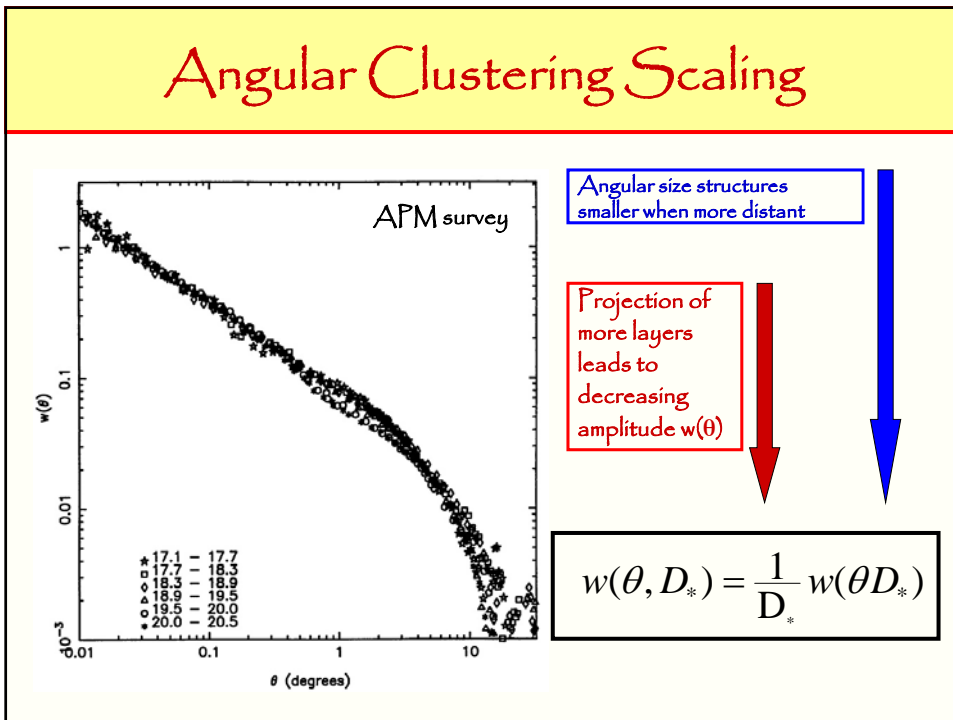
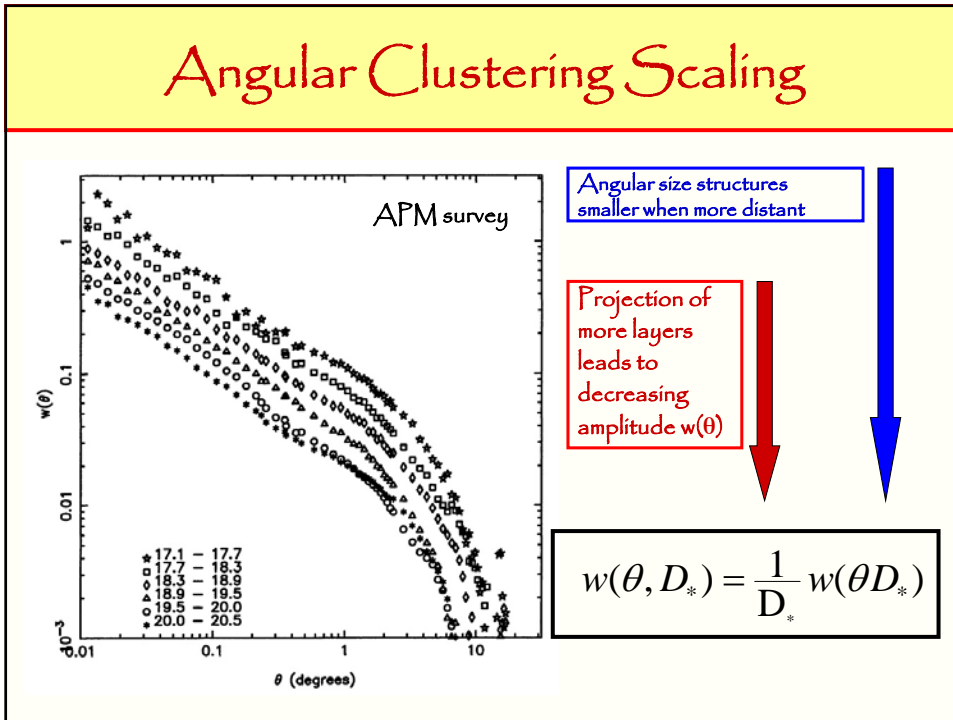
$$\gamma \approx 0.8$$

- large angles $\rightarrow 0$
ie. to homogeneity

Angular Clustering Scaling



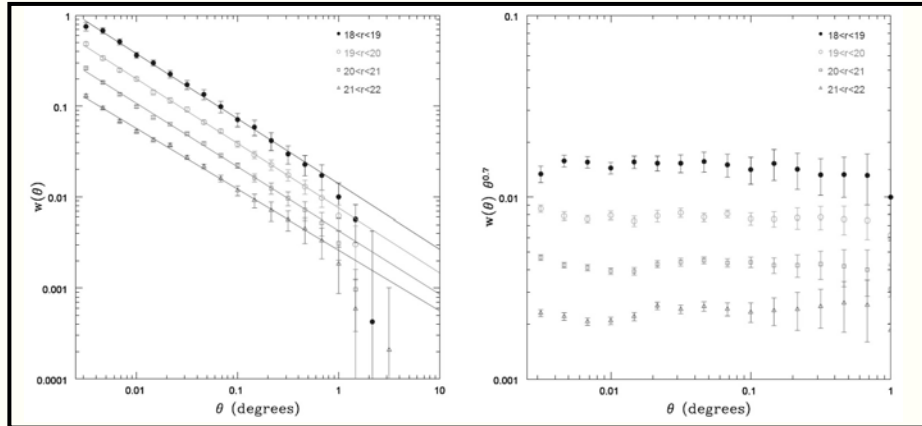
Projection of more layers leads to decreasing amplitude $w(\theta)$



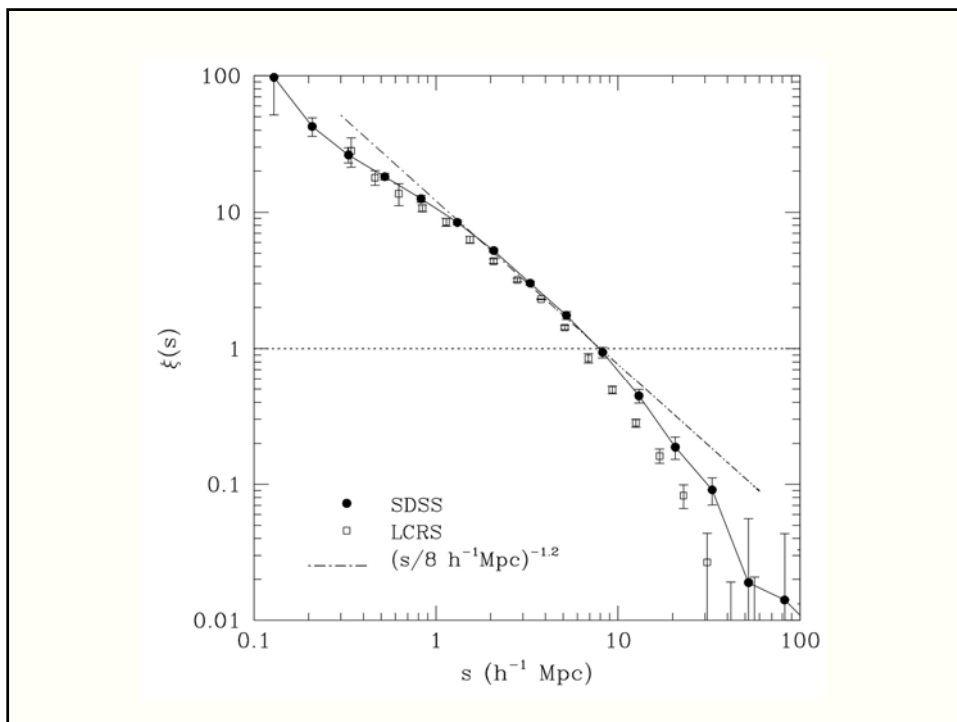
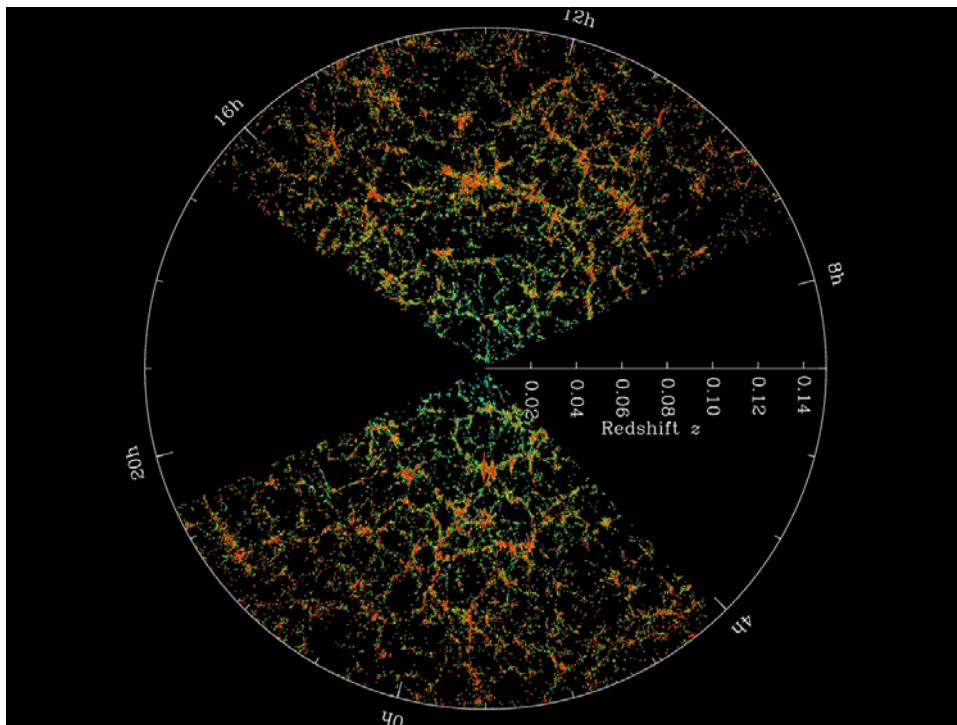
Angular Clustering Scaling

The angular scaling of $w(\theta)$ is found back to even fainter magnitudes in the SDSS survey ($m=22$)

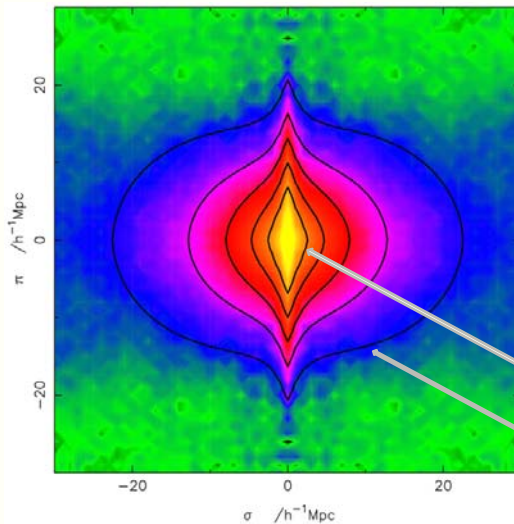
Clear evidence that there are no significant large structures on scales $> 100\text{--}200\text{ Mpc}$



Correlation Functions:
Redshift Space



sky-redshift space 2-pt correlation function $\xi(\sigma, \pi)$



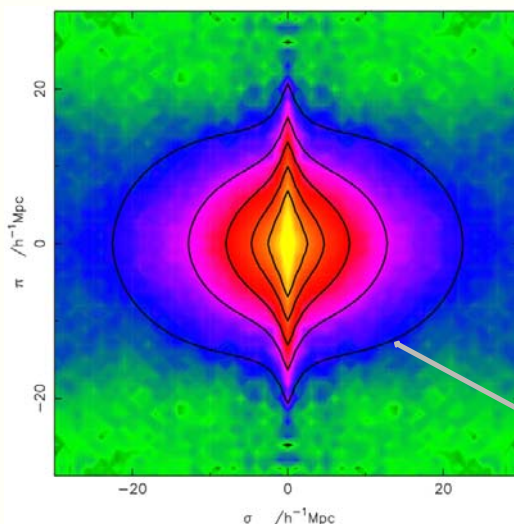
Correlation function determined in sky-redshift space:

$$\xi(\sigma, \pi)$$

sky position: $\sigma = (\alpha, \delta)$
redshift coordinate: $\pi = cz$

Close distances:
distortion due to non-linear
Finger of God
Large distances:
distortions due to large-scale
flows

Redshift Space Distortions Correlation Function



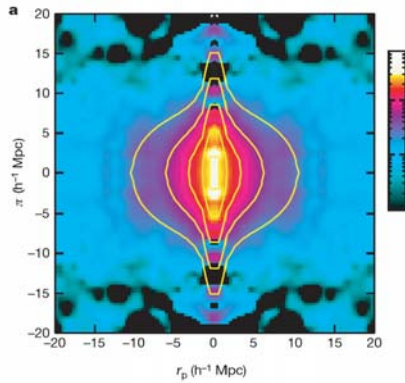
On average, $\xi_s(s)$ gets amplified wrt. $\xi_r(r)$

Linear perturbation theory (Kaiser 1987):

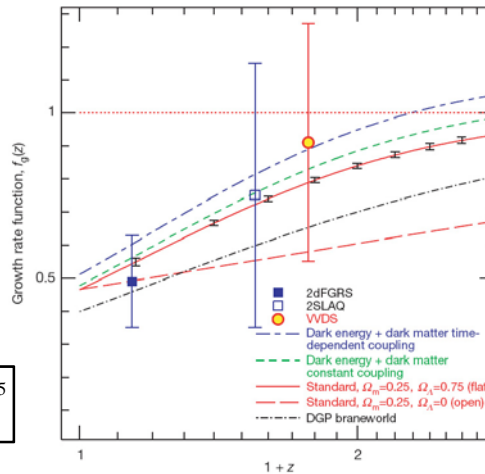
$$\xi_s(s) = \left(1 + \frac{2}{3}\Omega^{0.6} + \frac{1}{5}\Omega^{1.2}\right)\xi_r(s)$$

Large distances:
distortions due to large-scale
flows

Evolution Growth Rate



Linder 2008
Guzzo et al. 2008



$$f(\Omega_m, \Omega_\Lambda) = \frac{a}{D} \frac{dD}{da} \approx \Omega_m^{0.55}$$

Peebles growth rate factor

Measurement

Spatial 2pt-Correlation Function

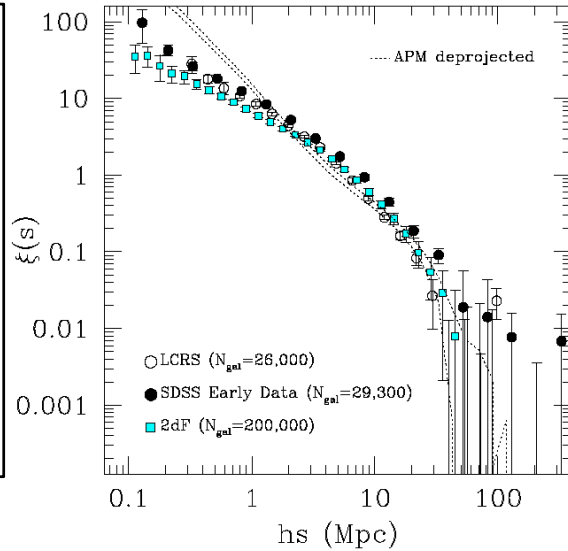
Deprojected Spatial Correlations

2pt correlation function
not an ideal power-law:

Halo Model:

Two-point correlation function
combination of

- 1) small-scale correlations,
due to galaxies inside
one dark matter halo
- 2) large scale correlations
between dark matter halos

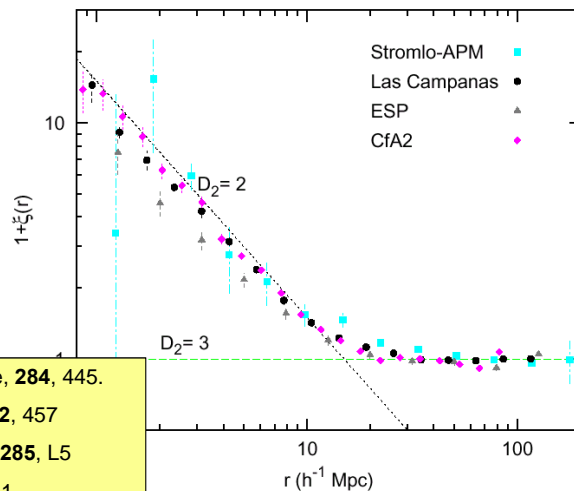


Convergence to Homogeneity

The correlation function
 $g(r)=1+\xi(r)$

Stromlo-APM, Las Campanas
CfA2, ESP redshift surveys.

The fractal behavior at small
scales disappears at larger
distances, providing evidence
for a gradual transition to
homogeneity.

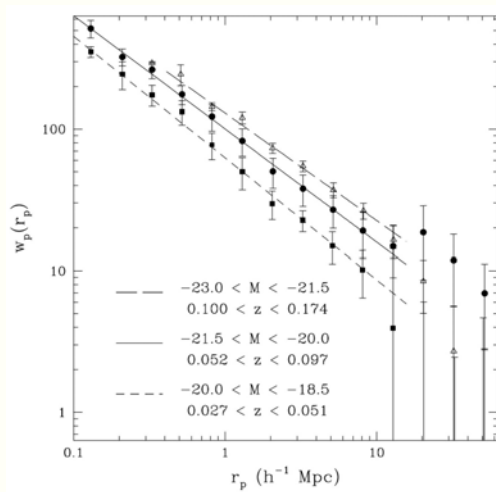


Plot from Martínez, 1999, *Science*, **284**, 445.

- (1) Loveday *et al.*, 1995, *ApJ*, **442**, 457
- (2) Tucker *et al.*, 1997, *MNRAS*, **285**, L5
- (3) Guzzo *et al.*, 2000, *AA*, **355**, 1

Luminosity Dependence Correlation Functions

Galaxy Luminosity Dependence



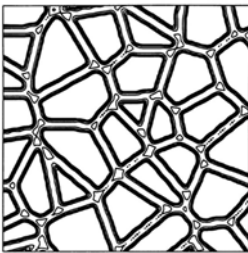
SDSS
correlation function

for galaxies in different
luminosity bins

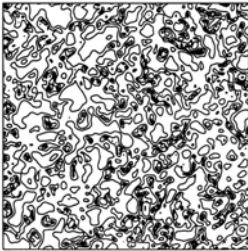
Spatial Structure & Correlation Functions

Structural Insensitivity

Voronoi foam, $R=1.6$, smoothed original



Voronoi foam, $R=1.6$, random phases



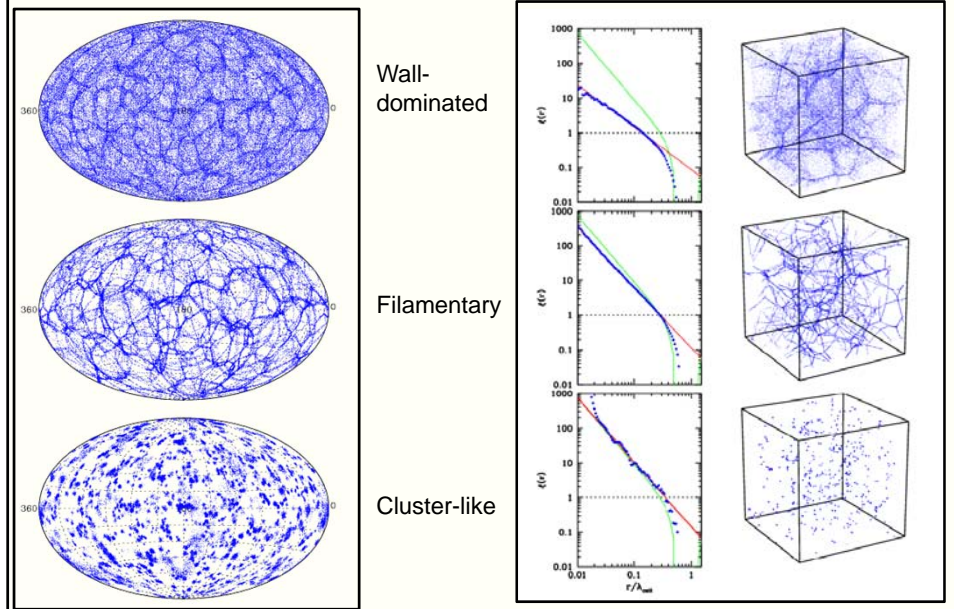
2-pt correlation function is highly insensitive to the geometry & morphology of weblike patterns:

compare 2 distributions with same $\xi(r)$, cq , $P(k)$, but totally different phase distribution

In practice, some sensitivity in terms of distinction Field, Filamentary, Wall-like and Cluster-dominated distributions:

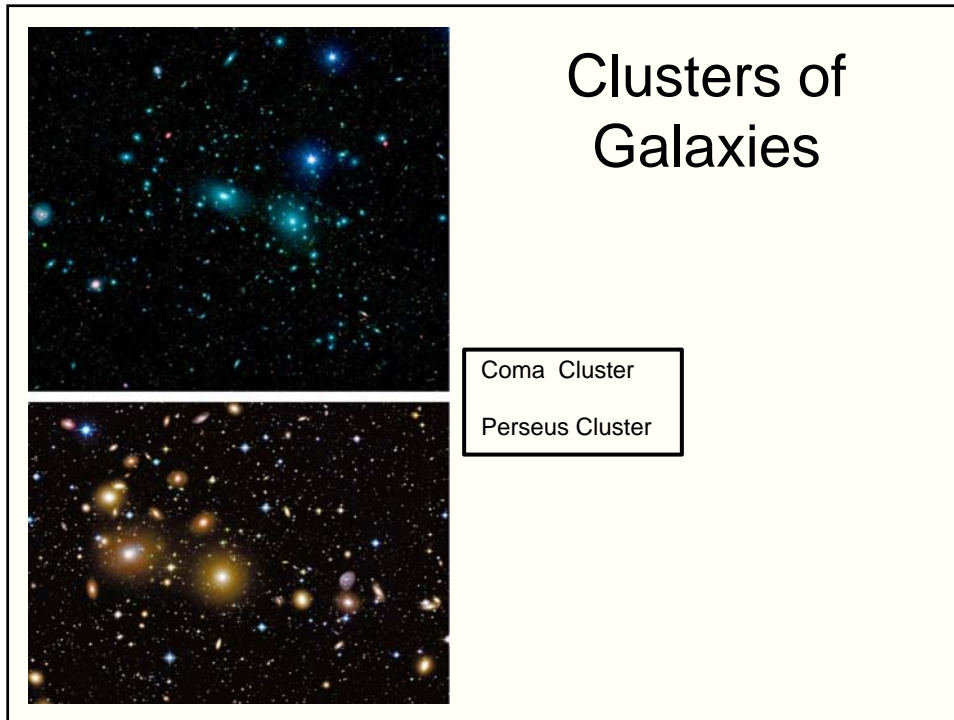
because of different fractal dimensions

Structural Sensitivity



Cluster

Correlation Functions

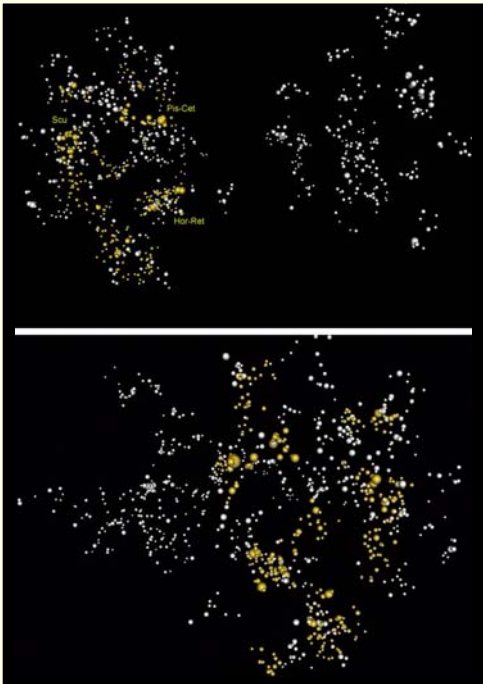


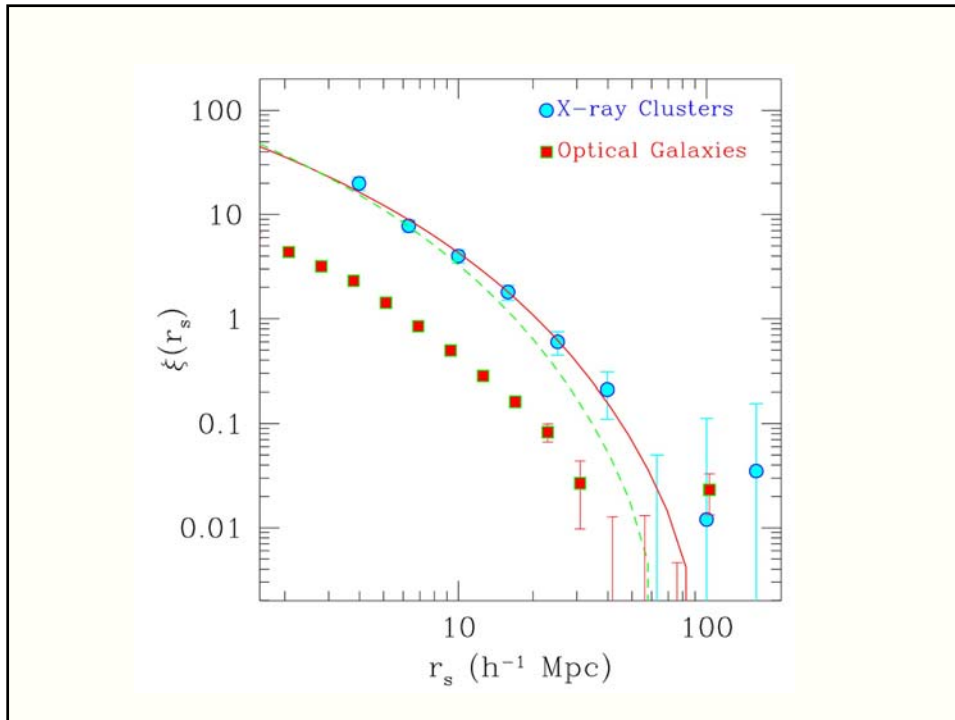
Clustering of Clusters

Clusters cluster much more strongly than galaxies:

- clustering defines superclusters !
- also power-law 2-pt correlation fct.
- same power law slope $\gamma \sim 1.8$
- much higher correlation length r_0 :

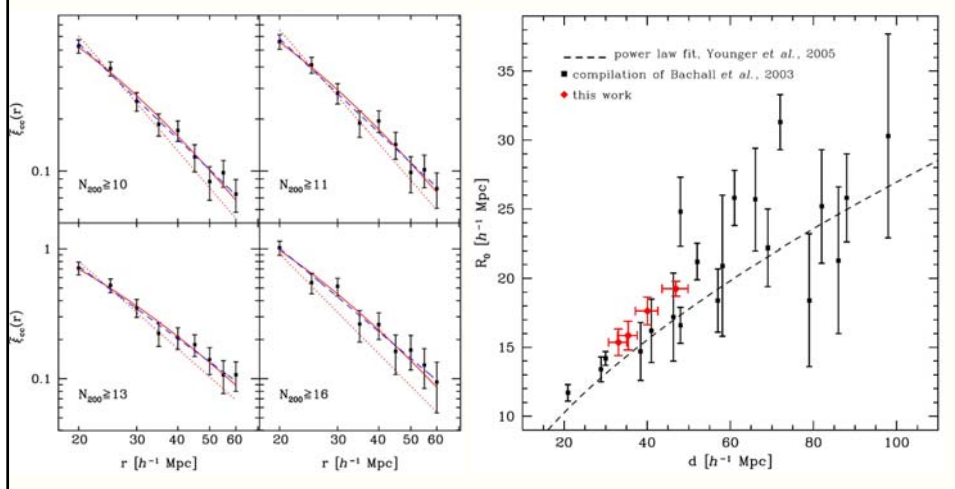
$r_0 \sim 15-25 \text{ h}^{-1} \text{ Mpc}$





Richness-Dependent Cluster Correlations

More massive clusters are systematically more strongly clustered than lower mass ones.



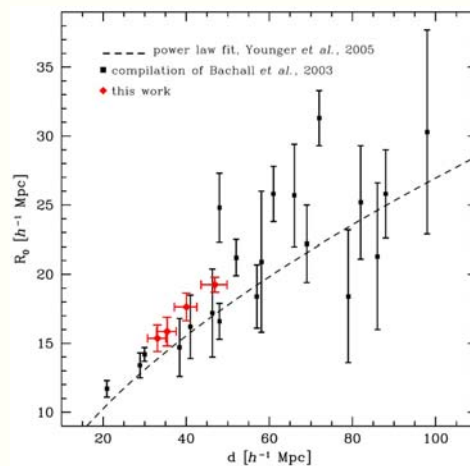
Richness-Dependent Cluster Correlations

More massive clusters are more systematically more strongly clustered than lower mass ones:

simple model:
Szalay & Schramm 1985

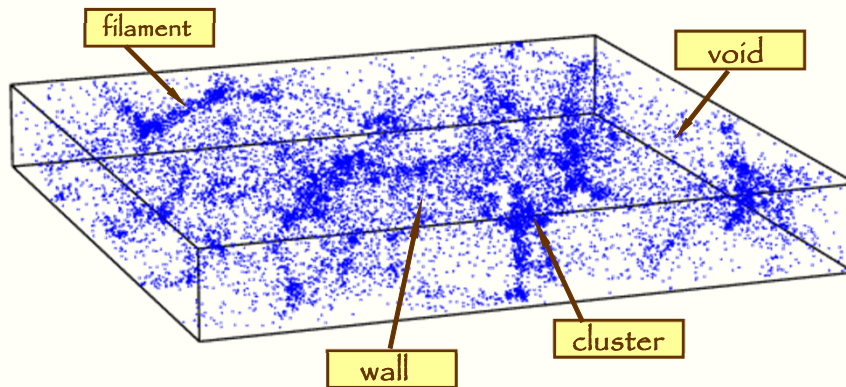
$$\xi_{cc}(r) = \beta \left(\frac{L(r)}{r} \right)^\gamma$$

$$L(R) = n^{-1/3}$$

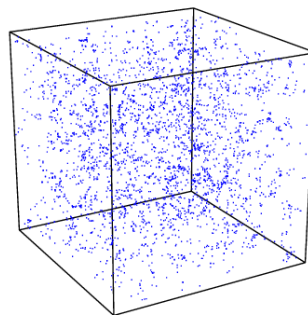


Scaling of
Cluster Correlation Functions:
a geometric model

Voronoi Models: Templates for the Cosmic Web

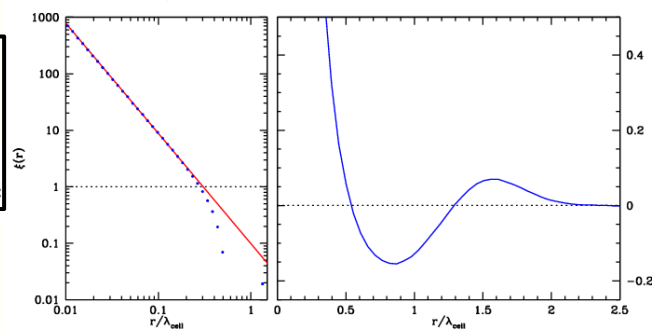


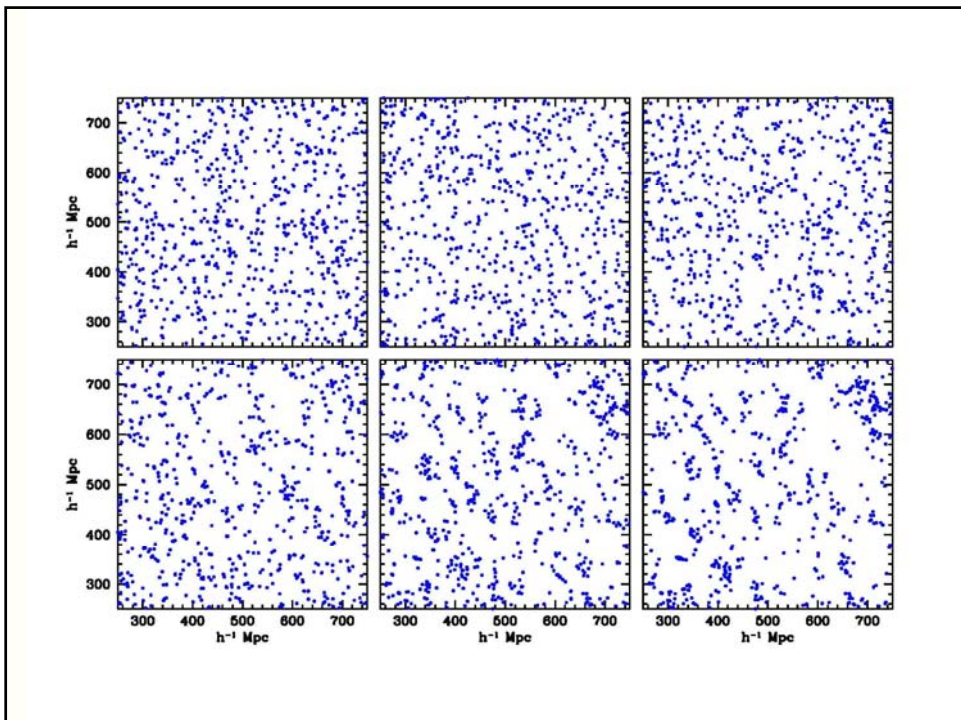
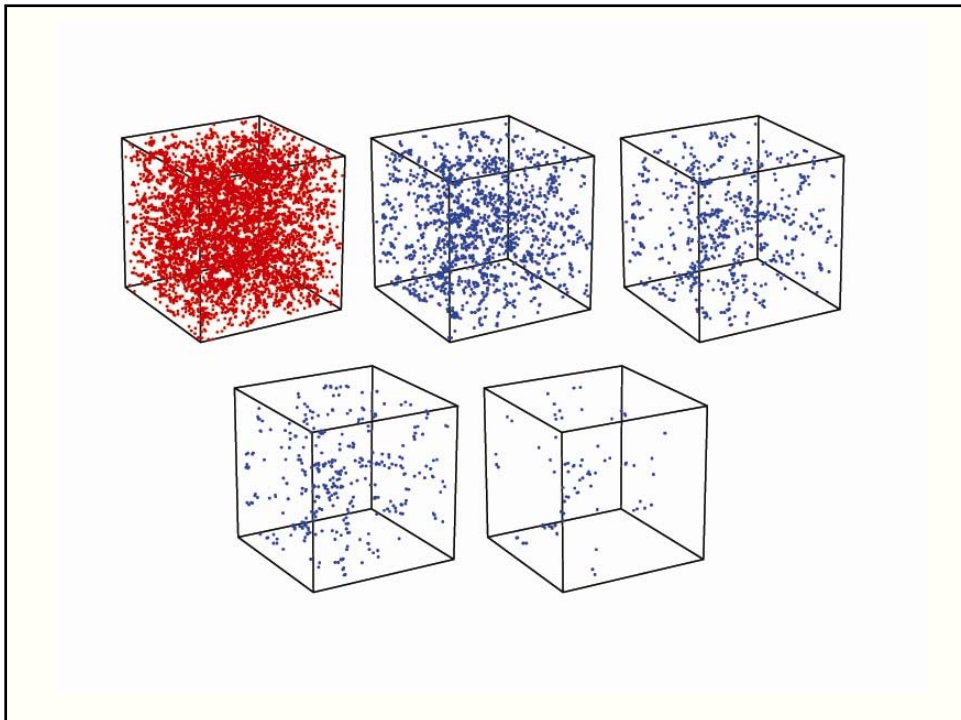
Perfect
Power-law clustering
Voronoi vertices



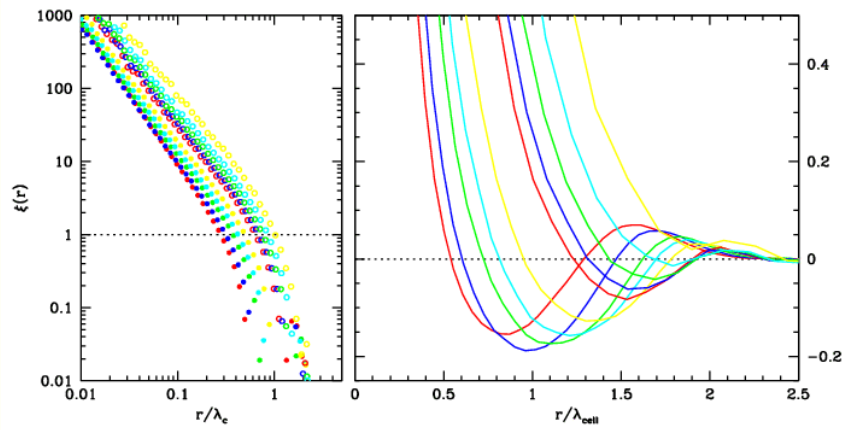
$$\xi_{vv}(r) = \left(\frac{r_0}{r}\right)^\gamma$$

$\gamma = 1.95; \quad r_0 \approx 0.3 \lambda_c$



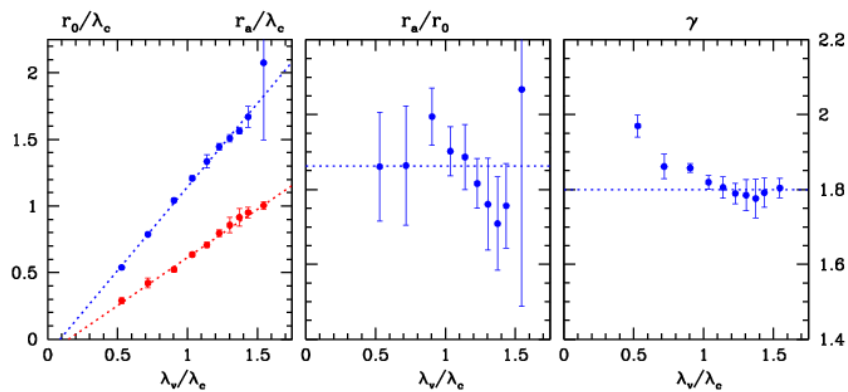


Self-similar Clustering



As function of mass, the correlation length r_0 and coherence length r_a increase unanimously.

Self-similar Clustering



As function of mass, the correlation length r_0 and coherence length r_a increase unanimously.

Higher Order Correlation Functions:

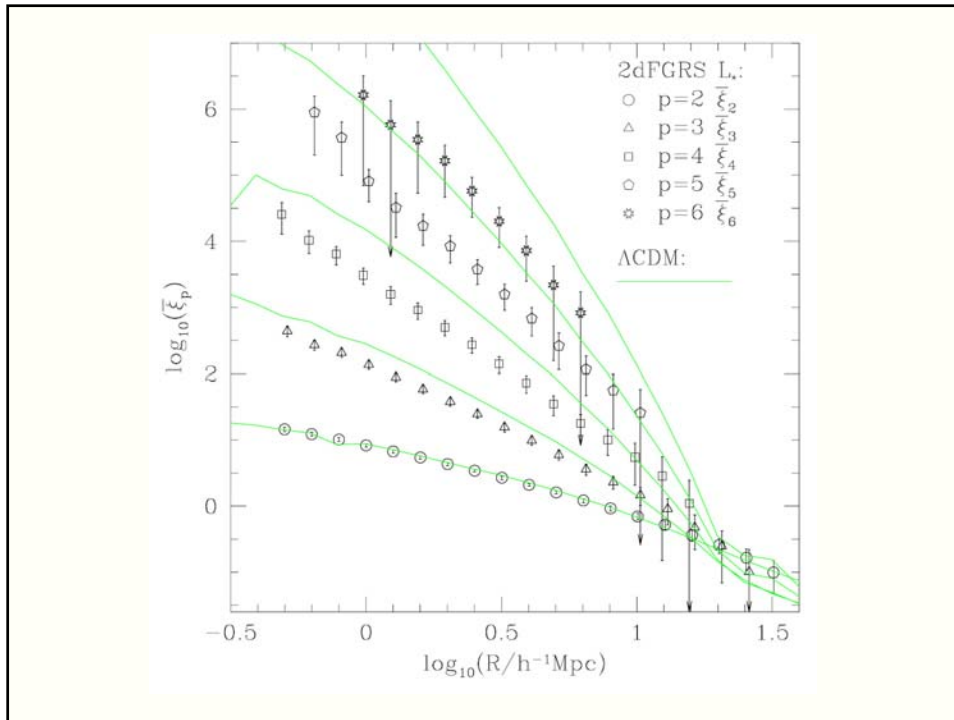
N-point correlation functions

- N-point correlation function

$$\xi^{(n)}(\vec{x}_1, \vec{x}_2, \dots, \vec{x}_n)$$

- Probability function of finding an n-tuplet of galaxies in n specified volumes dV_1, dV_2, \dots, dV_n

$$dP(\vec{x}_1, \vec{x}_2, \dots, \vec{x}_n) = \bar{n}^n [1 + \xi^{(n)}] dV_1 dV_2 \dots dV_n$$



3-point correlation functions

3-point correlation function

$$dP(\vec{x}_1, \vec{x}_2, \vec{x}_3) = \bar{n}^{-3} [1 + \xi^{(3)}] dV_1 dV_2 dV_3$$

$$[1 + \xi^{(3)}] = \left\langle \prod_i (1 + \delta_i) \right\rangle$$



$$[1 + \xi^{(3)}] = 1 + \xi(r_{12}) + \xi(r_{13}) + \xi(r_{23}) + \zeta(\vec{r}_1, \vec{r}_2, \vec{r}_3)$$

3-point correlation functions

3-point correlation function

$$[1 + \xi^{(3)}] = 1 + \xi(r_{12}) + \xi(r_{13}) + \xi(r_{23}) + \zeta(\vec{r}_1, \vec{r}_2, \vec{r}_3)$$

reduced 3-point correlation function

$$\zeta(\vec{r}_1, \vec{r}_2, \vec{r}_3) = \langle \delta_1 \delta_2 \delta_3 \rangle$$

excess correlation over that described by the 2-pt contributions

- $\zeta \neq 0$: non-Gaussian density field
- Hierarchical ansatz (Groth & Peebles 1977)

$$\zeta(\vec{r}_1, \vec{r}_2, \vec{r}_3) = Q(\xi_{12}\xi_{23} + \xi_{23}\xi_{31} + \xi_{31}\xi_{12})$$

Power Spectrum

Power Spectrum

- Directly measuring clustering in Fourier space:
 - More intuitive physically:
 - separating processes on different scales
 - Theoretical model predictions are made in terms of power spectrum
 - Amplitudes for different wavenumbers are statistically orthogonal

Power Spectrum $P(k)$

$$\delta(\mathbf{x}) = \int \frac{d\mathbf{k}}{(2\pi)^3} \hat{\delta}(\mathbf{k}) e^{-i\mathbf{k}\cdot\mathbf{x}}$$

$$\begin{aligned} (2\pi)^3 P(k_1) \delta_D(\mathbf{k}_1 - \mathbf{k}_2) &\equiv \langle \hat{f}(\mathbf{k}_1) \hat{f}^*(\mathbf{k}_2) \rangle \\ &\Updownarrow \\ P(k) &\propto \langle \hat{f}(\mathbf{k}) \hat{f}^*(\mathbf{k}) \rangle \end{aligned}$$

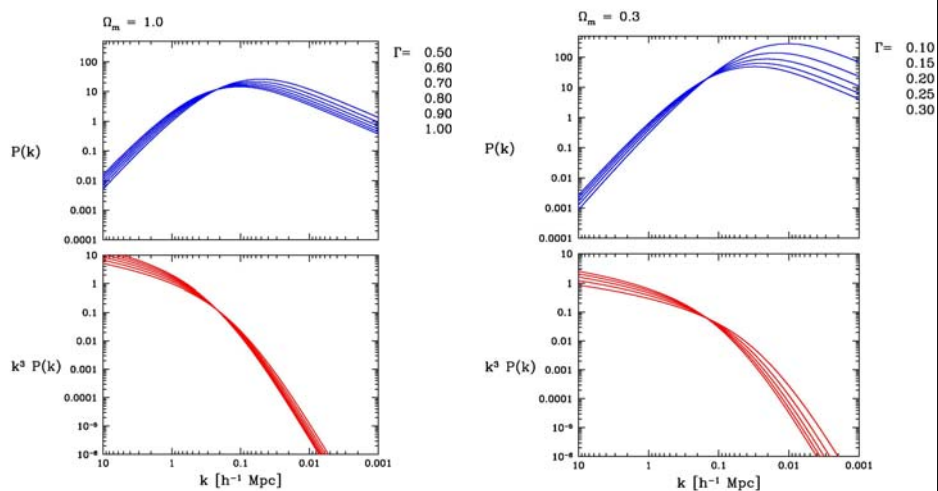
CDM Power Spectrum $P(k)$

$$P_{\text{CDM}}(k) \propto \frac{k^n}{[1 + 3.89q + (16.1q)^2 + (5.46q)^3 + (6.71q)^4]^{1/2}} \times \frac{[\ln(1 + 2.34q)]^2}{(2.34q)^2}$$

$$q = k/\Gamma$$

$$\Gamma = \Omega_{m,0} h \exp\left\{-\Omega_b - \frac{\Omega_b}{\Omega_{m,0}}\right\}$$

Power Spectrum $P(k)$



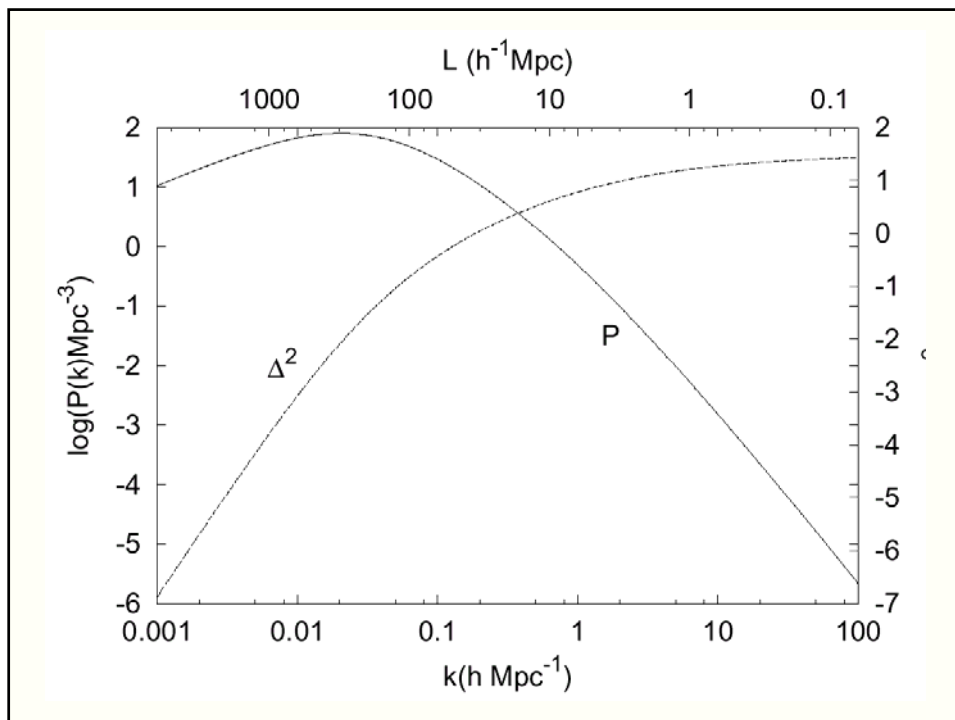
Power Spectrum - Correlation Function

$$P(k) = \int d^3r \xi(\vec{r}) e^{i\vec{k}\cdot\vec{r}}$$

$$\xi(\vec{r}) = \int \frac{d^3k}{(2\pi)^3} P(k) e^{-i\vec{k}\cdot\vec{r}}$$

Isotropy: $\xi(r) = 4\pi \int_0^\infty \frac{k^2 dk}{(2\pi)^3} P(k) \frac{\sin(kr)}{kr}$

Delta-power $\Delta^2(k) = \frac{1}{2\pi^2} P(k) k^2$



Power Spectrum Estimators

Estimators of $P(k)$

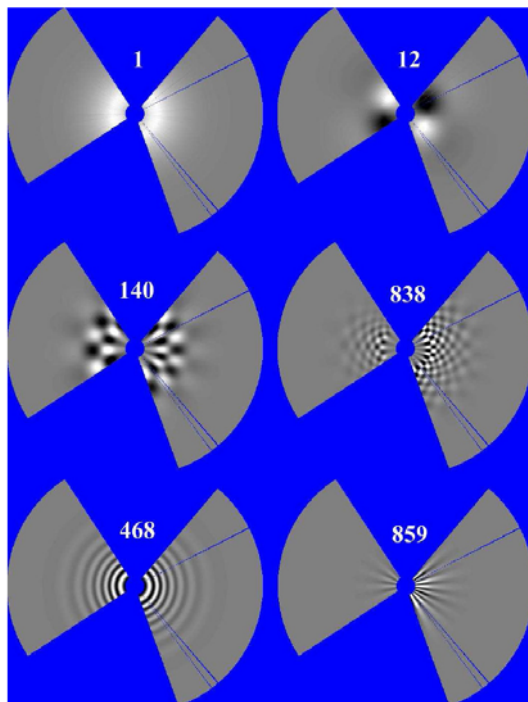
- Direct estimator
- Pixelization and maximum likelihood
- Karhunen-Loève (signal-to-noise) transform
- Quadratic compression
- Bayesian
- Multiresolution decomposition

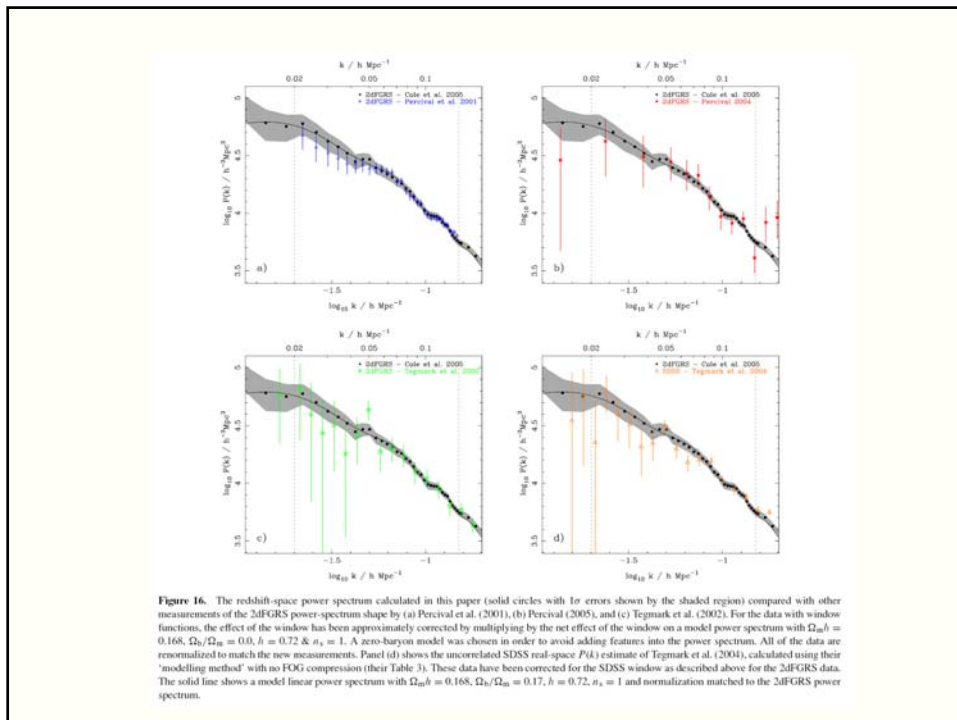
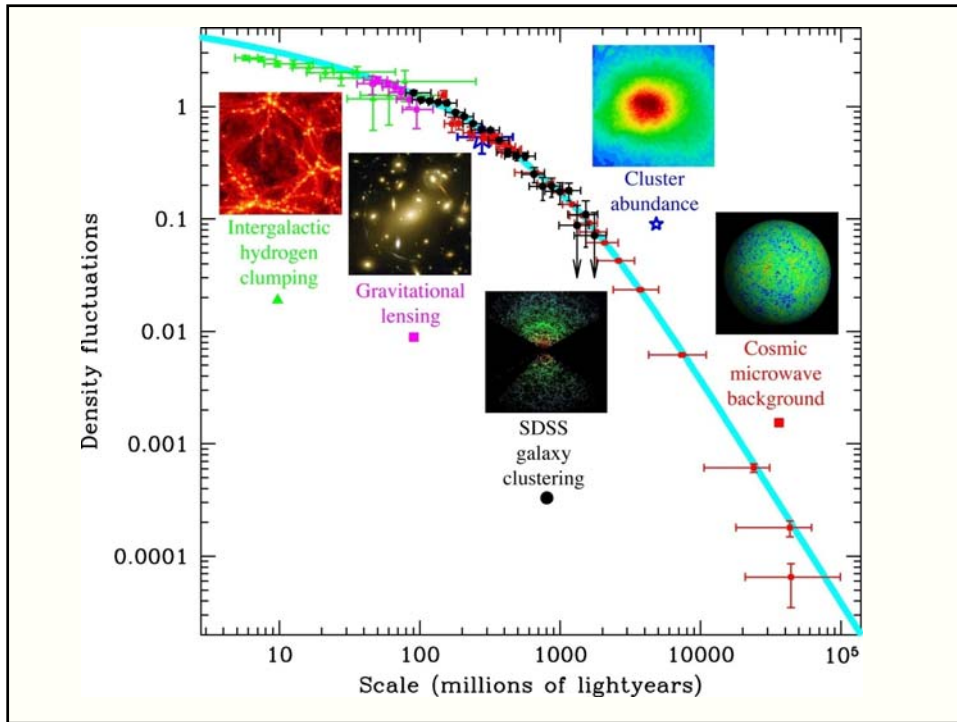
Tegmark, Hamilton, Strauss, Vogeley, and Szalay, (1998),
Measuring the galaxy power spectrum with future redshift
surveys, ApJ, **499**, 555

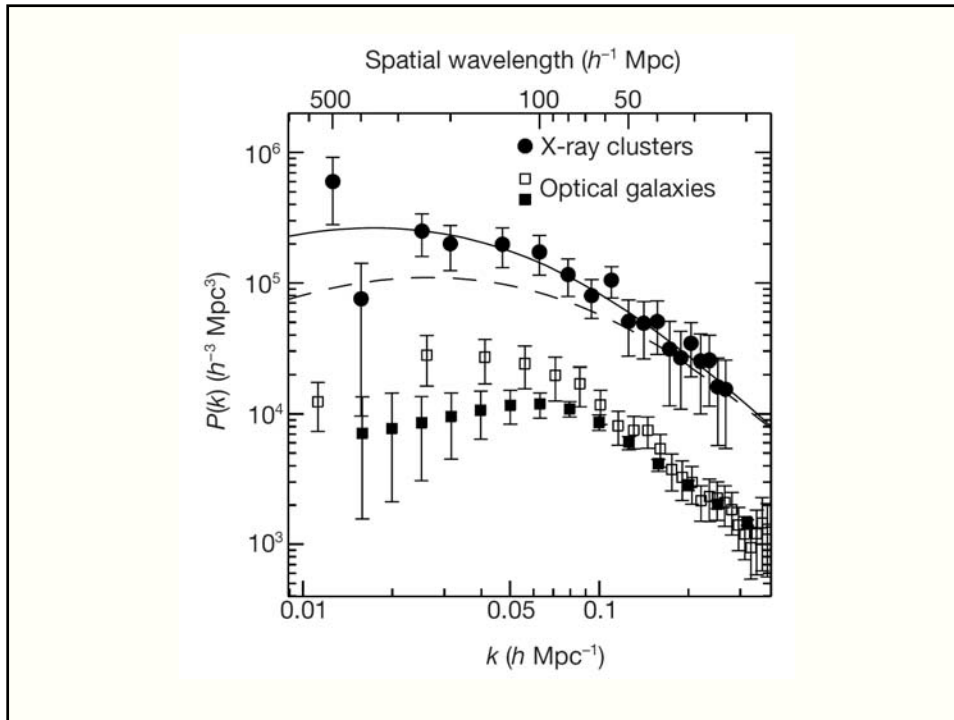
Karhunen-Loeve

Decomposition in series of
orthogonal
signal-noise eigenfunctions

Vogeley & Szalay 1995

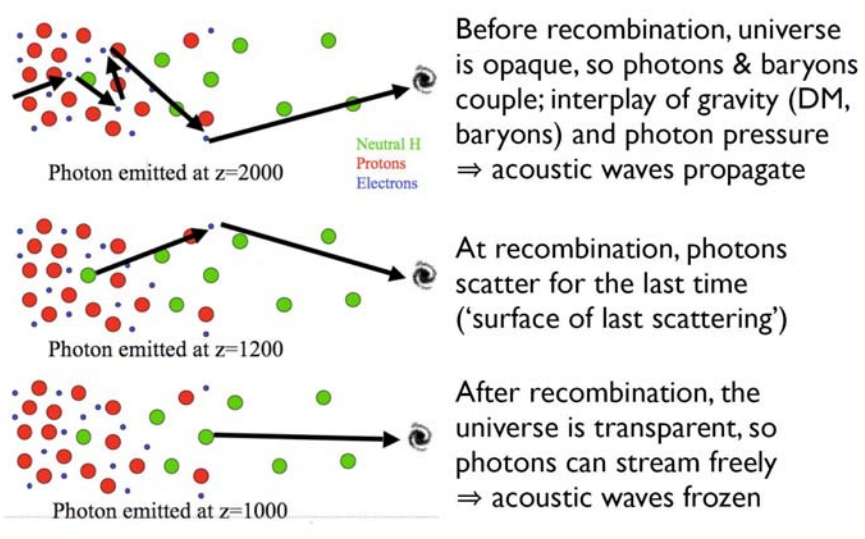




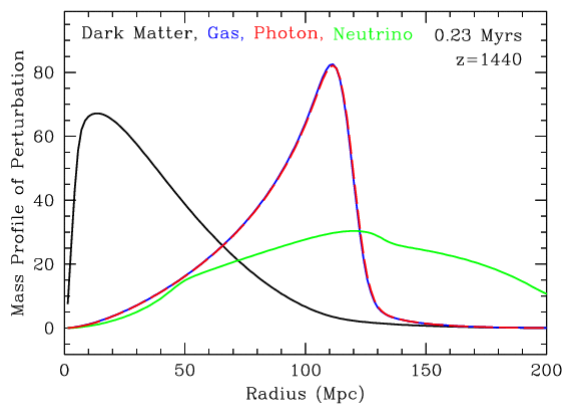


Baryonic Acoustic
Oscillations

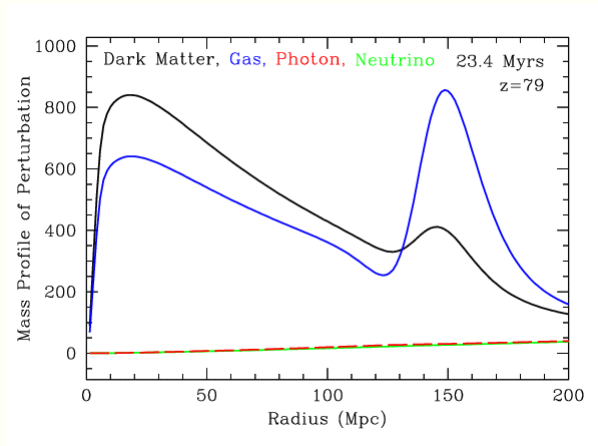
BAO



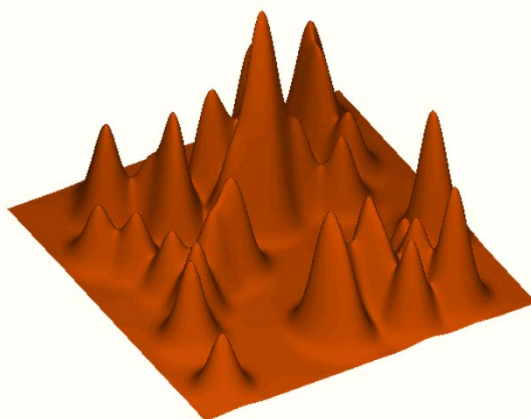
BAO



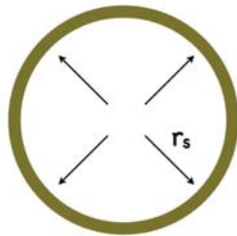
BAO



Measuring BAO

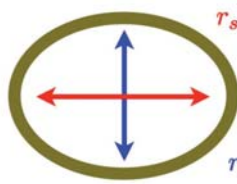


BAO as cosmological tools



Until recombination, the sound wave travels a distance of:

$$r_s = \int_{z_{rec}}^{\infty} \frac{c_s(z)}{H(z)} dz$$

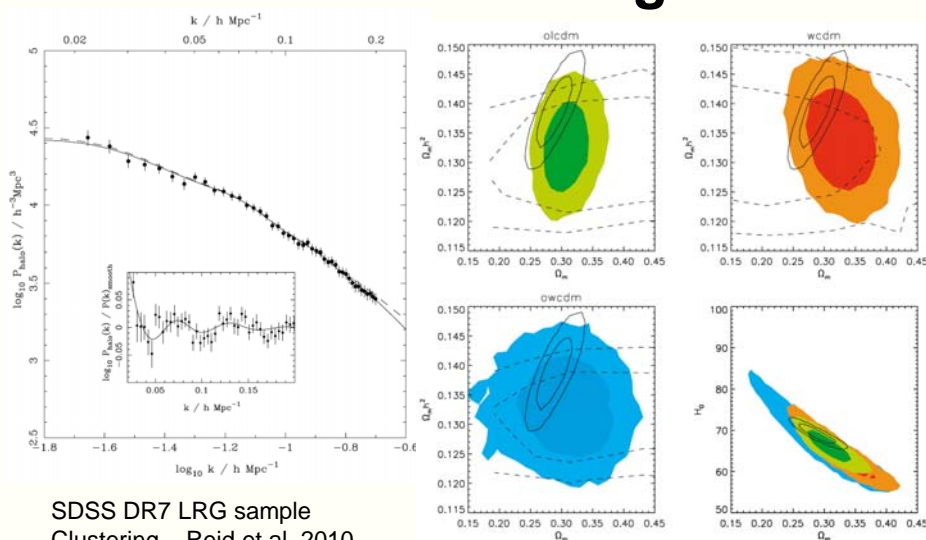


$$r_s = D_A(z) \Delta\theta$$

$$r_s = \frac{c}{H(z)} \Delta z$$

This distance can be accurately determined from the CMB power spectrum, and was found to be 147 ± 2 Mpc.

Cosmic Constraints LSS Clustering



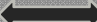
Topological Analysis of the Cosmic Web

Cosmic Structure Analysis

To assess the

key aspects of the

nonlinear cosmic matter and galaxy distribution:

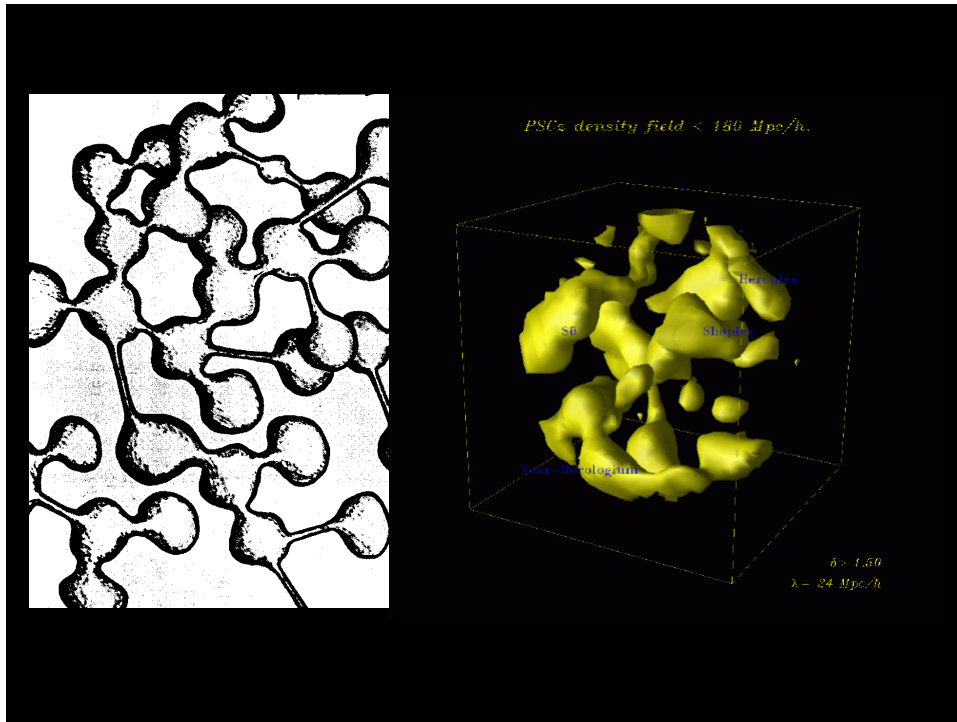
- | | | |
|---|---|--|
| <ul style="list-style-type: none"> • multiscale character • weblike network • volume dominance voids |  | <ul style="list-style-type: none"> hierarchical structure formation anisotropic collapse asymmetry overdense vs. underdense |
|---|---|--|

Many statistical measures:

clustering measures (correlation functions)
density distribution functions

Topological Characteristic of network:
Geometric Characteristics:

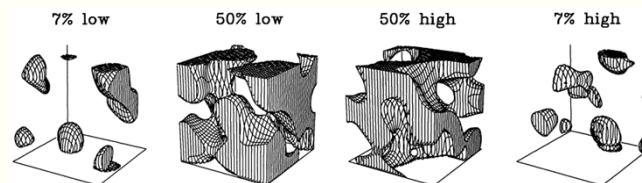
genus statistics
Minkowski functionals



Why is the topology study useful?

1. Direct intuitive meanings

- characterize the LSS as a quantitative measure with a physical interpretation attached



2. Easy to measure

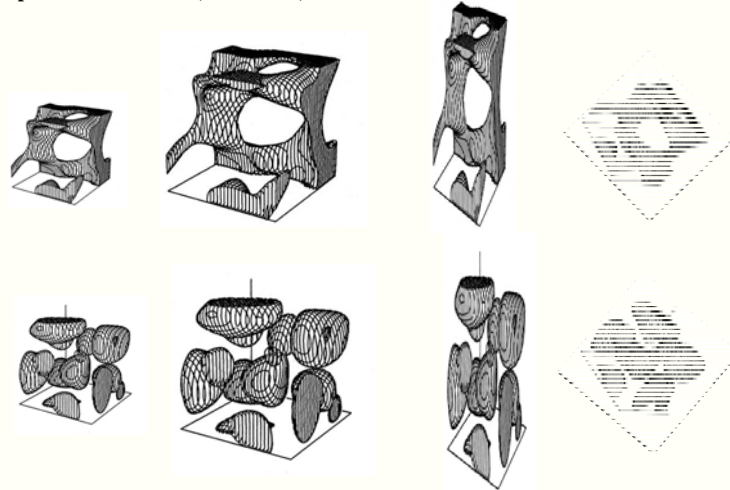
- global genus topology from integration of local curvature:

According to the Gauss-Bonnet theorem the integrated Gaussian curvature of a surface is related with its topological genus by

$$C = \int K dA = 4\pi(1 - G)$$

Intrinsic topology

does not change by trivial change in the shape of structure or by trivial coordinate transformation, which result in monotonic expansion/contraction, distortion, rotation ...



II. Introductory theory of topology statistics

Measures of intrinsic topology - **Minkowski Functionals**

3D

- 1. 3d genus (Euler characteristic)
- 2. mean curvature
- 3. contour surface area
- 4. volume fraction

→ 3d galaxy redshift survey data, 3d HI map

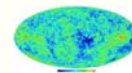


II. Introductory theory of topology statistics
 1. Measures of intrinsic topology
 2. Definitions of MFs
 3. Gaussian formulae

2D

- 1. 2d genus (Euler characteristic)
- 2. contour length
- 3. area fraction

→ CMB temp./polarization, 2d galaxy surveys



1D

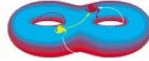
- 1. level crossings
- 2. length fraction

→ Ly α clouds, deep HI surveys, pencil beam galaxy surveys

Topological definition of the genus, $G = -V_3$

Genus = # of holes in iso-density contour surfaces - # of isolated regions

[ex. $G(\text{sphere}) = -1$, $G(\text{torus}) = 0$, $G(\text{two tori}) = +1$]



: 2 holes - 1 body = +1

The topological genus is related with the integrated Gaussian curvature of a surface by (Gauss-Bonnet theorem)

$$C = \int K dA = 4\pi(1 - G)$$

Gauss – Bonnet Theorem

For a surface with c components, the genus G specifies # handles on surface, and is related to the Euler characteristic $\chi(\partial M)$ via:

$$G = c - \frac{1}{2} \chi(\partial M)$$

where, according to the Gauss-Bonnet theorem, the Euler-Poincare characteristic is given by the surface integral over the Gaussian curvature

$$\chi(\partial M) = \frac{1}{2\pi} \oint \left(\frac{1}{R_1 R_2} \right) dS$$

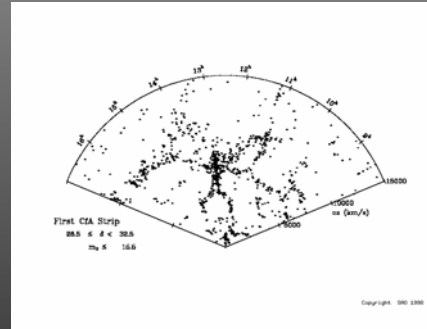
The usefulness of Euler

The mean value of χ can be calculated analytically for Gaussian random fields (test of GRF hypothesis?)

In 3D the mean level is characterised by $g > 0$ (a sponge)

In 2D the mean level has $\chi = 0$.

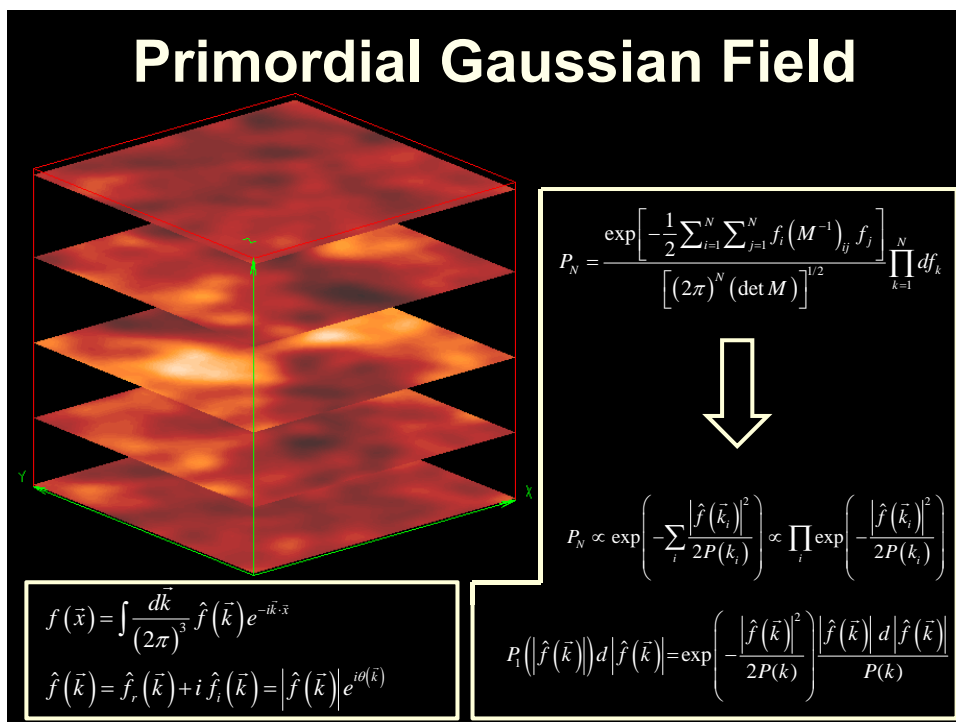
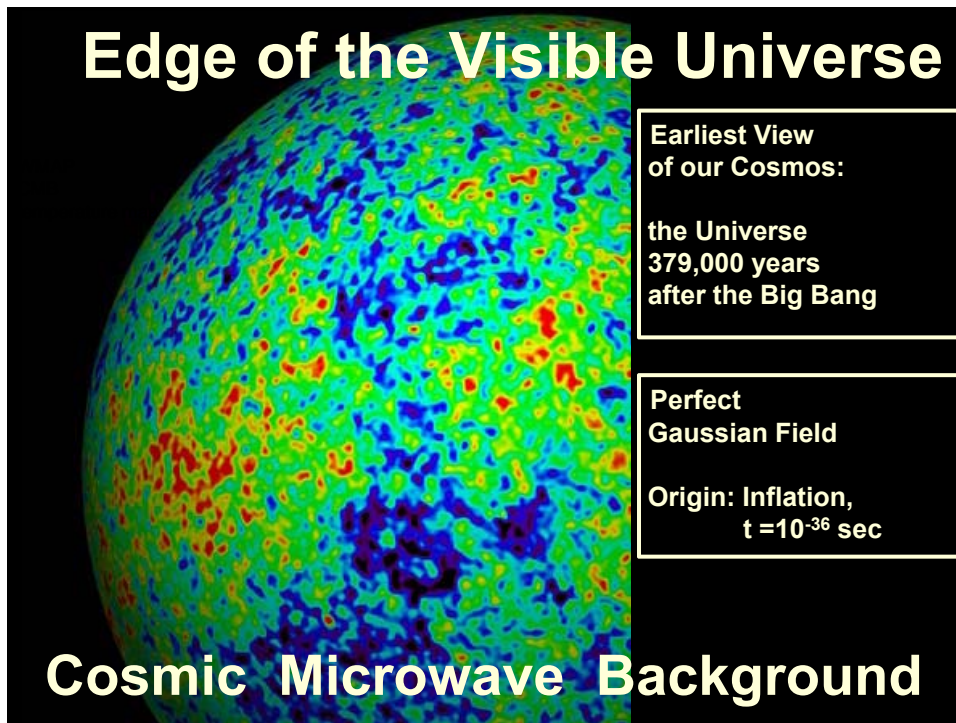
There is no 2D equivalent of a sponge!

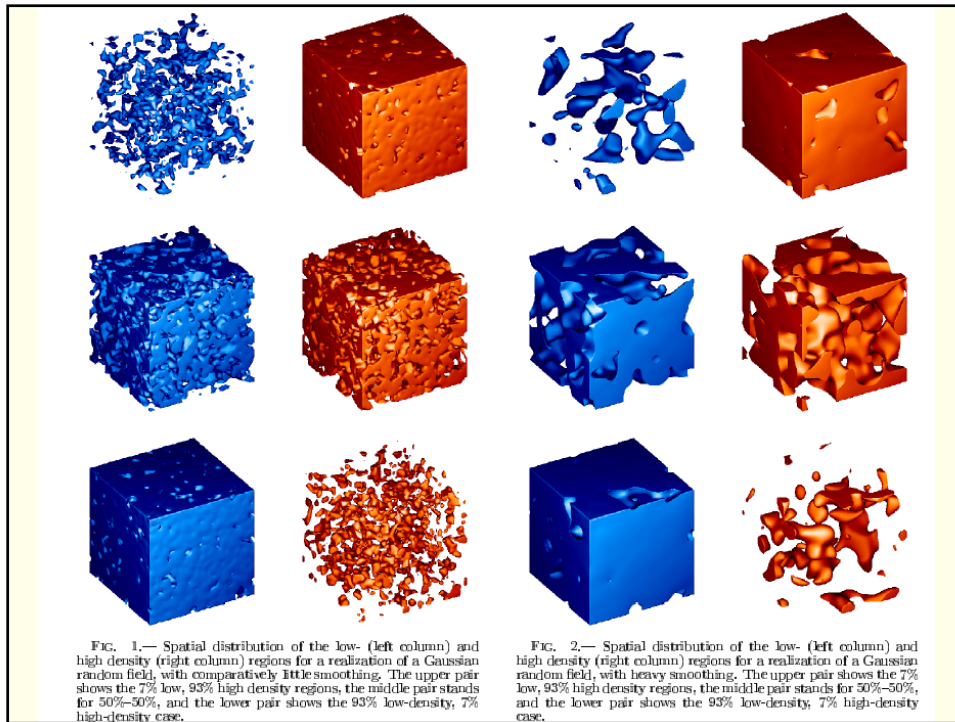


Topology

of the

Primordial Gaussian Field

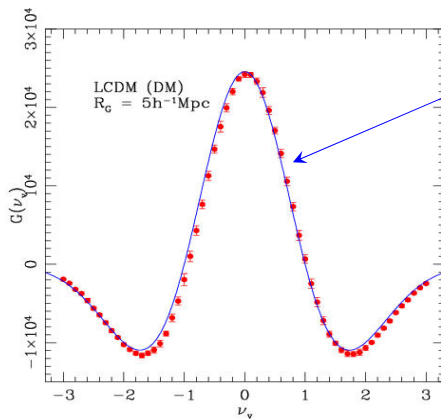




Gaussian Random Fields: Genus

Genus Gaussian Field, the “cosmological” way :

$$g = G - c$$

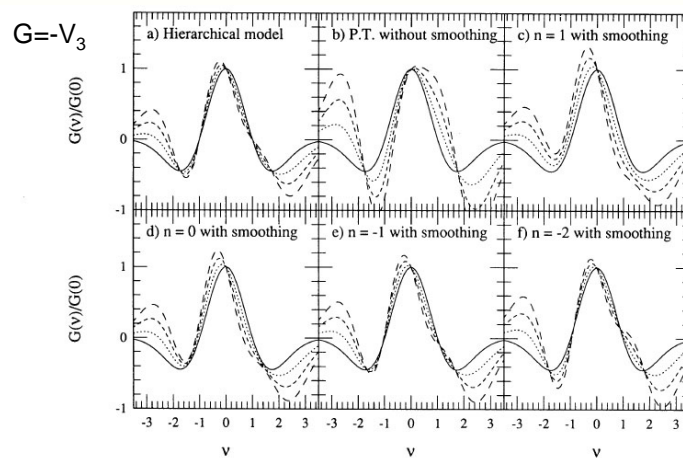


$$g(v) = -\frac{1}{8\pi^2} \left(\frac{\langle k^2 \rangle}{3} \right)^{3/2} (1-v^2) e^{-v^2/2}$$

$$g(v) = -\beta_0(v) + \beta_1(v) - \beta_2(v)$$

Topology of non-Gaussian Fields

Analytic formulae for the genus in weakly nonlinear regime due to gravitational evolution are known too (Matsubara 1994). So the non-Gaussianity due to non-linear gravitational evolution can be separated, and the primordial topology can be better explored.



Moore et al. (1992): The topology of the QDOT IRAS redshift survey
 The amplitude of the genus curves on large (21Mpc/h) scales is inconsistent with the predictions of a constant-bias SCDM model, and the shape of the best-fit PS from genus analysis is $n=-1$
 * IRAS QDOT: 2163 redshifts out to $z=0.07$, randomly sampled at a rate of 1/6 from IRAS PSC ($f_{60\mu m} > 0.6Jy$), $|b| > 10$

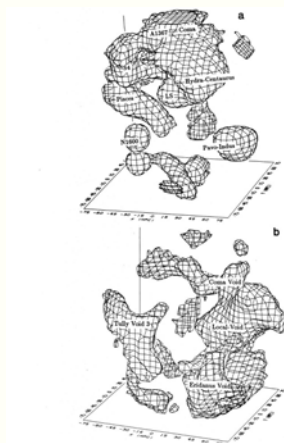


Figure 3. Randomly chosen in the QDOT survey including roughly one third of the total volume. The Galactic Centre points towards the right-hand side of the plot, along the positive x-axis, with galactic longitude increasing anticlockwise around the sphere. (a) High-density regions within a sphere of radius $75 h^{-1} Mpc$, identified with a Gaussian of width $\sigma = 12.5 h^{-1} Mpc$. (b) Low-density regions on the same scale and with the same orientation as in (a). (c) High-density regions to a depth of $100 h^{-1} Mpc$, identified on scale $\sigma = 25 h^{-1} Mpc$. (d) Low-density regions on the same scale and with the same orientation as in (c).

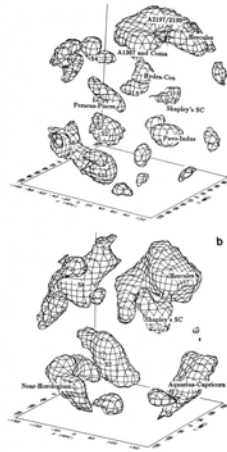


Figure 4. High-density regions of the QDOT survey. The coordinates are as in Fig. 3. (a) The high-density field of Fig. 3c) but at a higher resolution so that roughly only one tenth of the total volume is contained. (b) High-density regions, on the same volume as in (a), but at a higher resolution of $15 h^{-1} Mpc$, identified with $\sigma = 2.5 h^{-1} Mpc$. (c) and (d) The density field of Fig. 3c) at the resolution shown in (a) but at a grid down one half of the total volume. The structures are identifying and sparse like, as expected in a Gaussian random field.

Vogeley et al. (94): Topology Analysis of the CfA Redshift Survey
 Genus on $R_G = 4.2 \sim 14 Mpc/h$. Statistics derived from the genus curve
 Amplitude drop relative to the fields with the same PS due to phase correlation on scales $< 10 Mpc/h$
 → amplitude of the genus curve is not a good measure of n .
 The amplitude of the genus curves on large scales is inconsistent with the predictions of a constant bias SCDM, but consistent with a LCDM with $\Omega h = 0.24$ and $\Omega_\Lambda = 0.6$ and an OCDM with $\Omega h = 0.2$.
 * CfA2: ~ 12000 galaxies with $m_B < 15.5$.

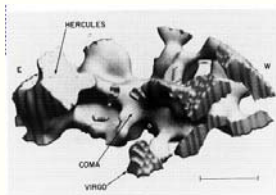


Fig. 3a

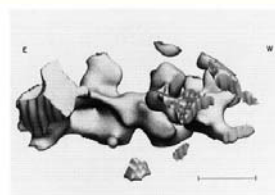


Fig. 3b

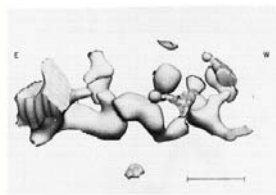


Fig. 3c

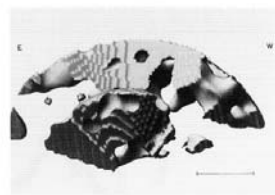
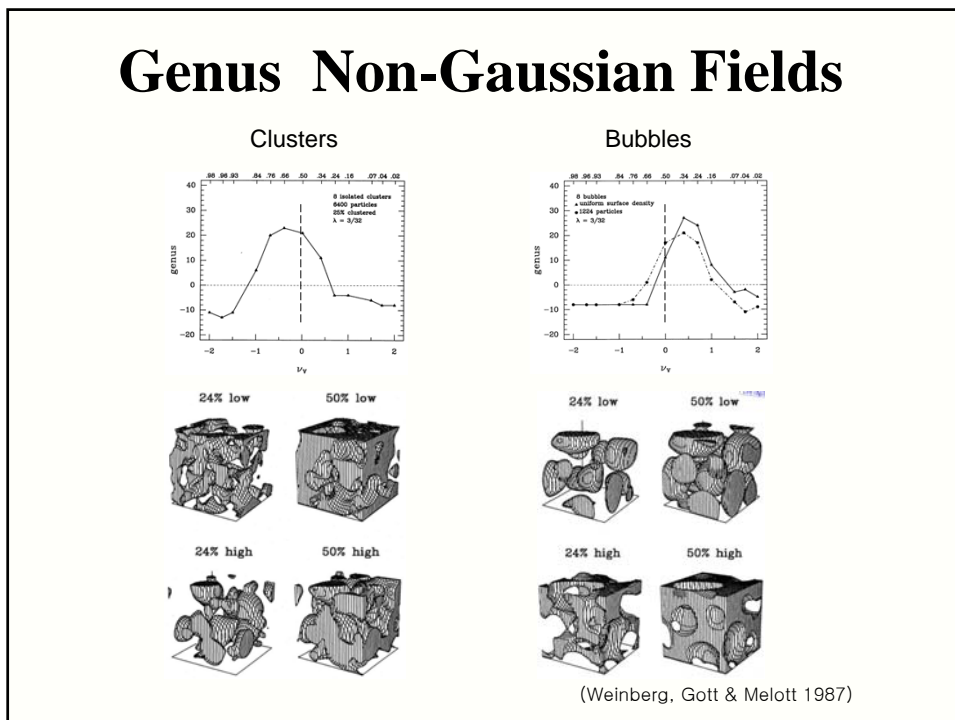
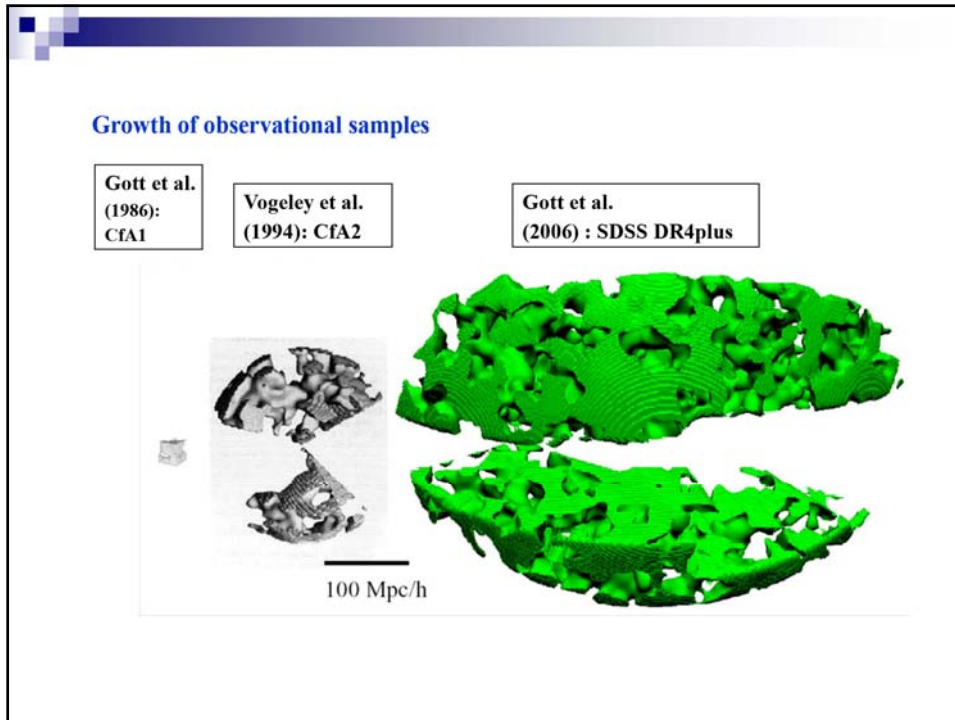


Fig. 3d



Minkowski Functionals

Minkowski Functionals

- Complete quantitative characterization of local geometry and morphology of isodensity surfaces in terms of

Minkowski Functionals

- Minkowski Functionals (defined by isodensity surface):

- Volume

$$V = \int dV$$

- Surface area

$$S = \oint dS$$

- Integrated mean curvature

$$C = \frac{1}{2} \oint \left(\frac{1}{R_1} + \frac{1}{R_2} \right) dS$$

- Integrated Intrinsic curvature
Euler Characteristic

$$\chi = \frac{1}{2\pi} \oint \left(\frac{1}{R_1 R_2} \right) dS$$

Minkowski Functionals: Non-Gaussianity Measure

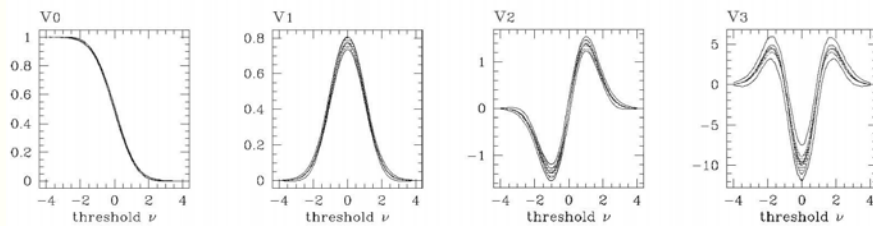
$$V_0(\nu) = \frac{1}{2} - \frac{1}{\sqrt{2\pi}} \int_0^\nu \exp(-x^2/2) dx$$

$$V_1(\nu) = \frac{2}{3} \frac{\lambda}{\sqrt{2\pi}} \exp(-x^2/2)$$

$$V_2(\nu) = \frac{2}{3} \frac{\lambda^2}{\sqrt{2\pi}} \nu \exp(-x^2/2)$$

$$V_3(\nu) = \frac{\lambda^3}{\sqrt{2\pi}} (\nu^2 - 1) \exp(-x^2/2)$$

Theoretical predictions for Gaussian fields are known.



$$\lambda^3 / \sqrt{2\pi} = \frac{1}{4\pi^2} \left(\frac{k^2}{3} \right)^{3/2}$$

(Schmalzing & Buchert 1997)

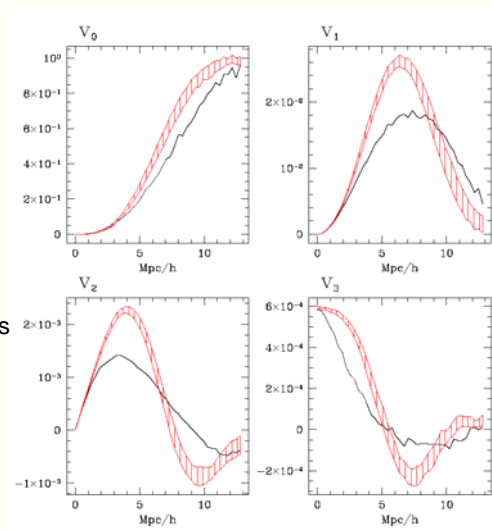
Minkowski functionals

In R^3 four functionals:

- volume V
- surface area A
- integral mean curvature H
- Euler-Poincare characteristic χ

These are the Minkowski Functionals

Kerscher & Martínez (1998),
Bull. Int. Statist. Inst. 57-2, 363



Homology Analysis of the Cosmic Web

Cosmic Structure Topology

- Complete quantitative characterization of homology in terms of

Betti Numbers

- Betti number β_k :
 - rank of homology groups H_p of manifold
 - number of k-dimensional holes of an object or shape

- 3-D object, e.g. density superlevel set:

β_0 :	- # independent components
β_1 :	- # independent tunnels
β_2 :	- # independent enclosed voids

Geometry & Topology

- Complete quantitative characterization of homology in terms of

Betti Numbers

- Complete quantitative characterization of local geometry in terms of

Minkowski Functionals

- Minkowski Functionals:
 - Volume
 - Surface area
 - Integrated mean curvature
 - Genus/Euler Characteristic

Genus, Euler & Betti

- Euler – Poincare formula

Relationship between Betti Numbers & Euler Characteristic χ :

$$\chi = \sum_{k=0}^d (-1)^k \beta_k$$

Genus, Euler & Betti

- Euler – Poincare formula

Relationship between Betti Numbers & Euler Characteristic χ .

3-D manifold \mathcal{M} :

$$\begin{aligned}\chi(M) &= \beta_0 - \beta_1 + \beta_2 + \beta_3 \\ &\approx \beta_0 - \beta_1 + \beta_2\end{aligned}$$

2-D boundary manifold $\partial\mathcal{M}$:

$$\chi(\partial M) = \beta_{0b} - \beta_{1b} + \beta_{2b}$$

Genus, Euler & Betti

- For a surface with c components, the genus G specifies # handles on surface, and is related to the Euler characteristic $\chi(\partial\mathcal{M})$ via:

$$G = c - \frac{1}{2} \chi(\partial M)$$

where, according to the Gauss-Bonnet theorem

$$\chi(\partial M) = \frac{1}{2\pi} \oint \left(\frac{1}{R_1 R_2} \right) dS$$

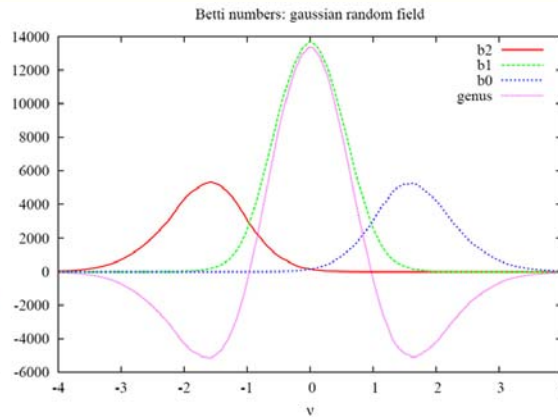
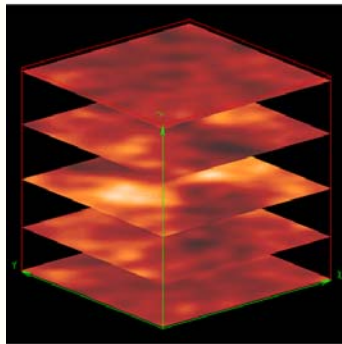
- Euler characteristic 3-D manifold \mathcal{M} & 2-D boundary manifold $\partial\mathcal{M}$:

$$\chi(M) = \frac{1}{2} \chi(\partial M)$$



$$\chi(M) = 2(\beta_0 - \beta_1 + \beta_2)$$

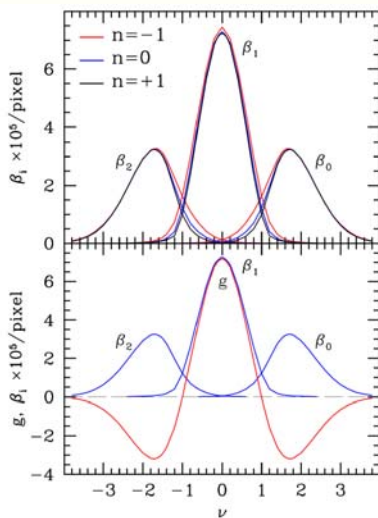
Gaussian Random Fields: Betti Numbers



In a Gaussian field:

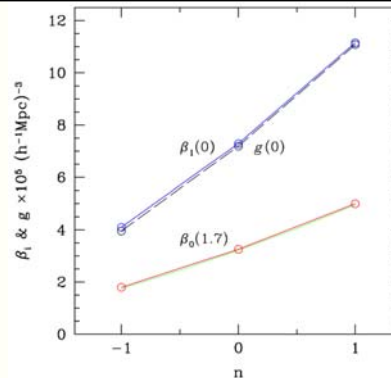
- # tunnels dominant at intermediate density levels, when superlevel domain spongelike
- overlap between β_0 and β_2 at $\nu=0$, domain punctured by clumps with cavities
- # clumps/islands reaches maximum at $\nu = \sqrt{3}$, # cavities/voids at $\nu = -\sqrt{3}$

Gaussian Random Fields: Betti Numbers

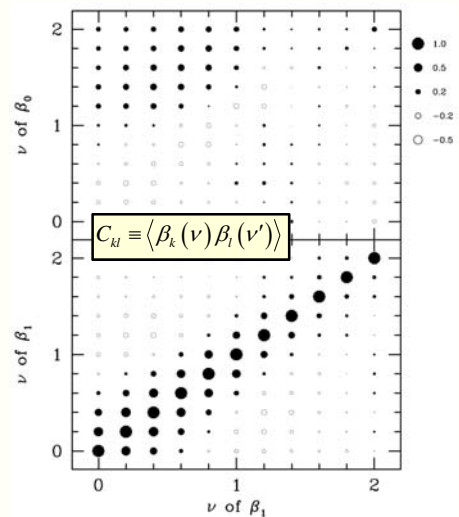
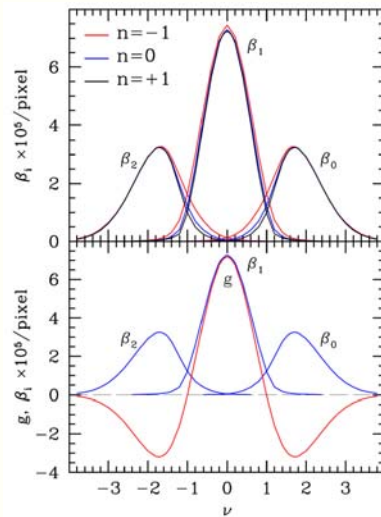


Distinct sensitivity of Betti curves on power spectrum $P(k)$:

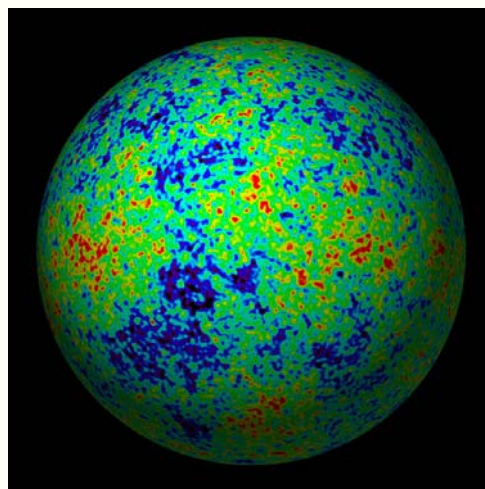
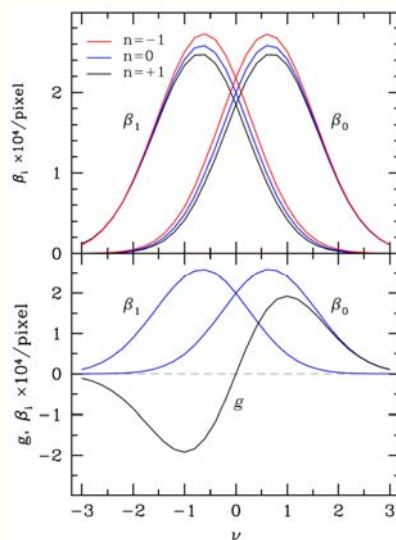
unlike genus (only amplitude $P(k)$ sensitive)



Gaussian Random Fields: Correlation Betti Numbers

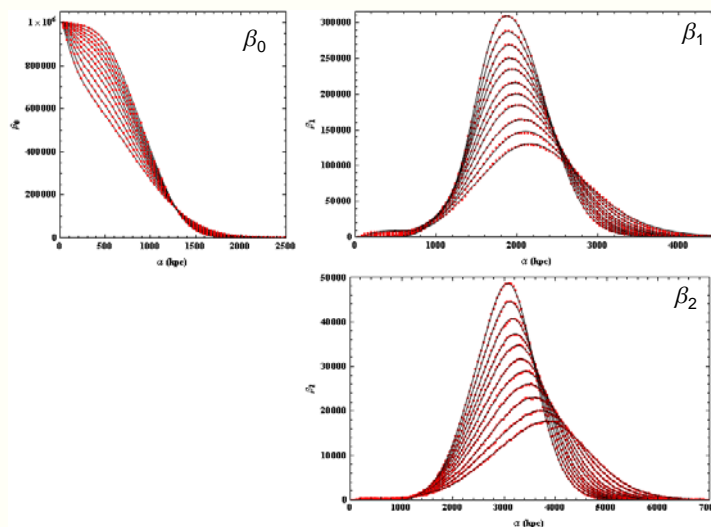


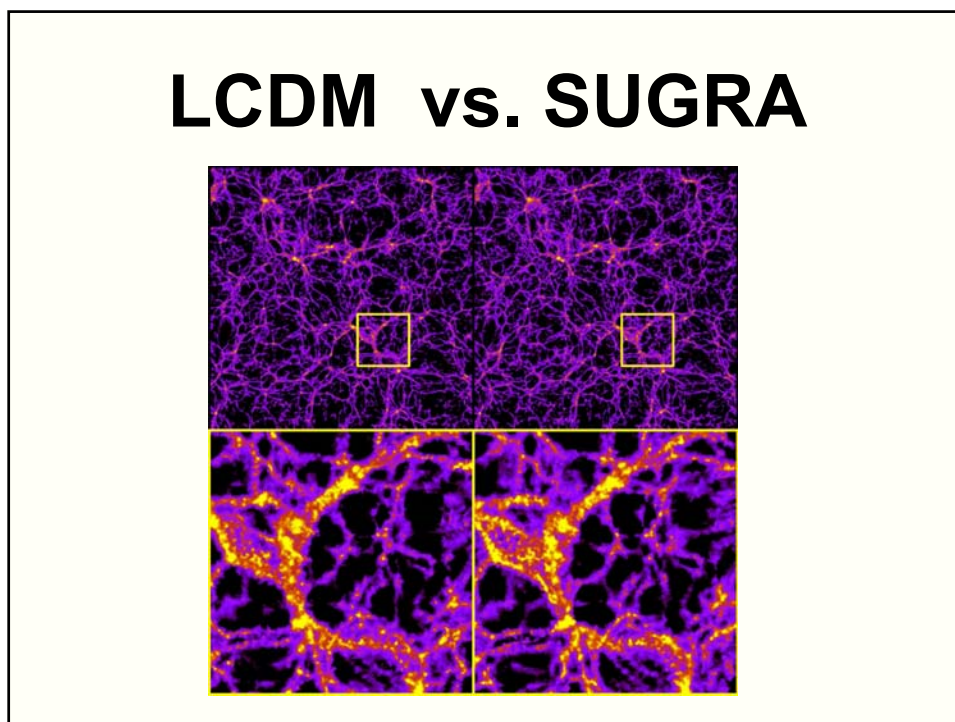
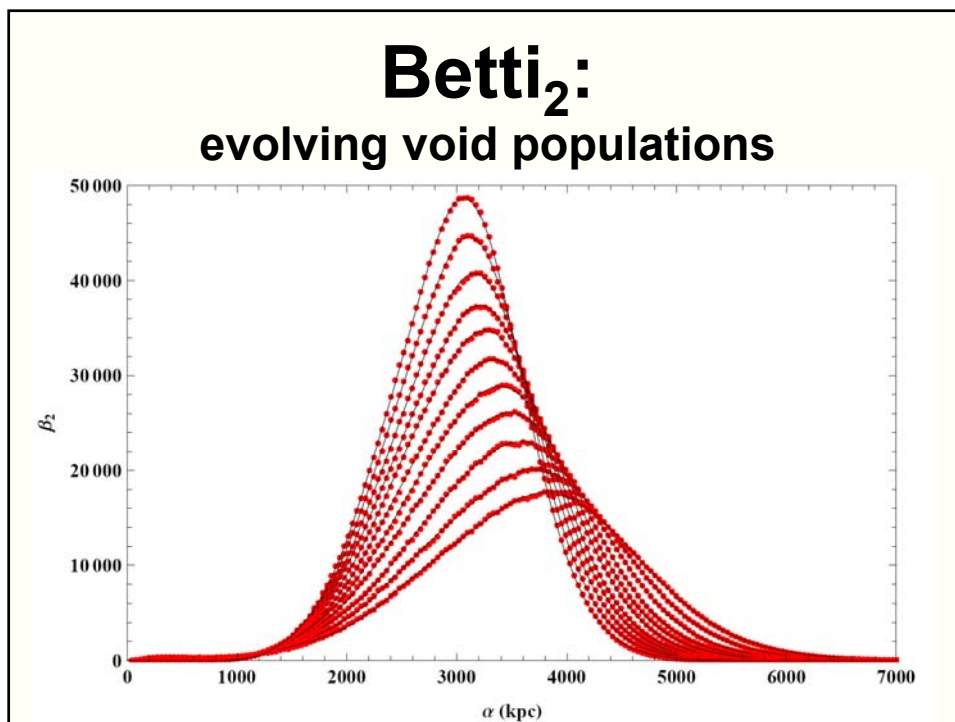
Gaussian Random Fields: Betti Numbers



Homology of the Cosmic Web

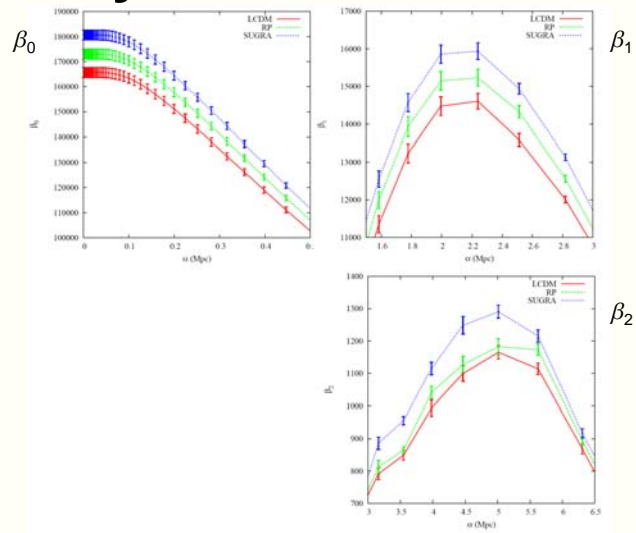
Homology of evolving LCDM cosmology





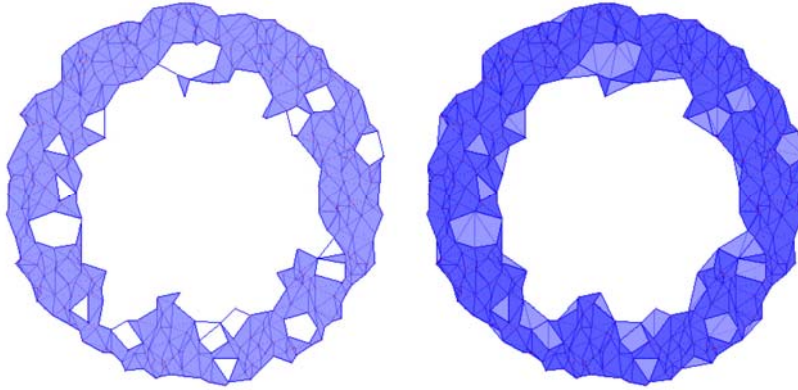
Homology

sensitivity LCDM vs. Quintessence



Persistence

Persistence: search for topological reality

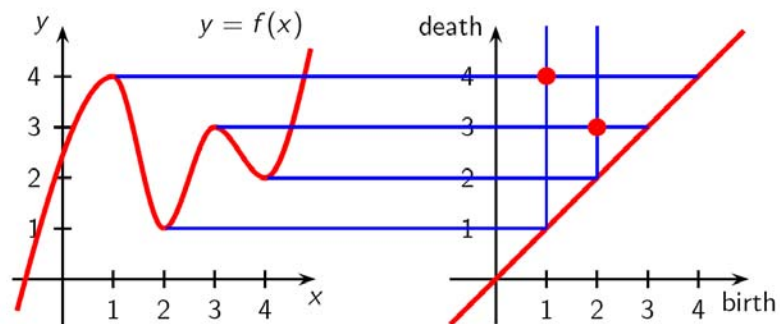


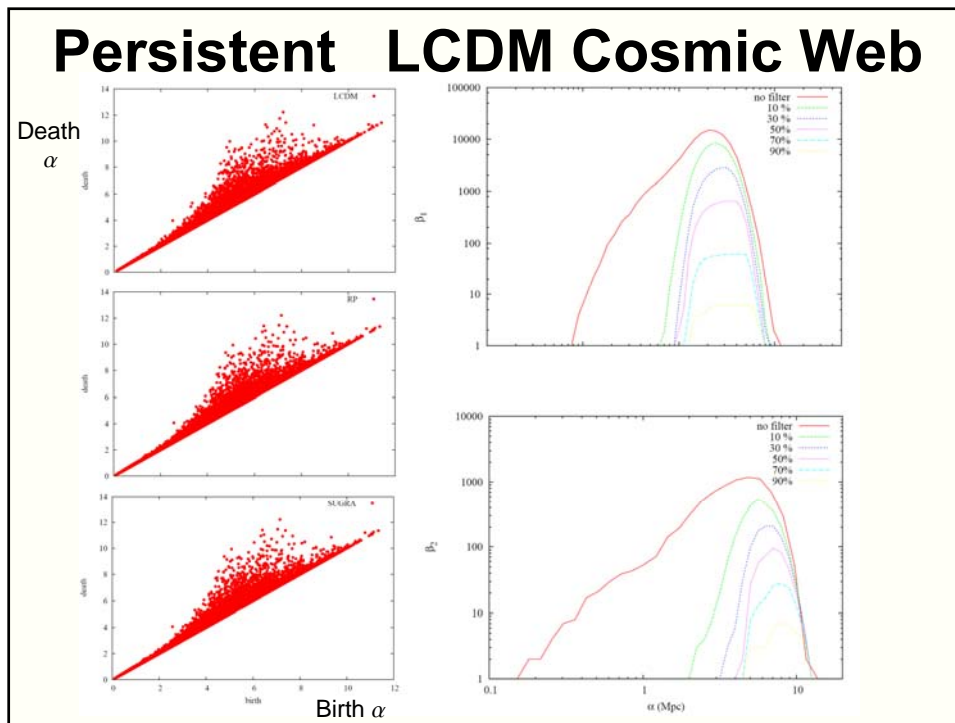
Concept introduced by Edelsbrunner:

Reality of features (eg. voids) determined on the basis of α -interval between "birth" and "death" of features

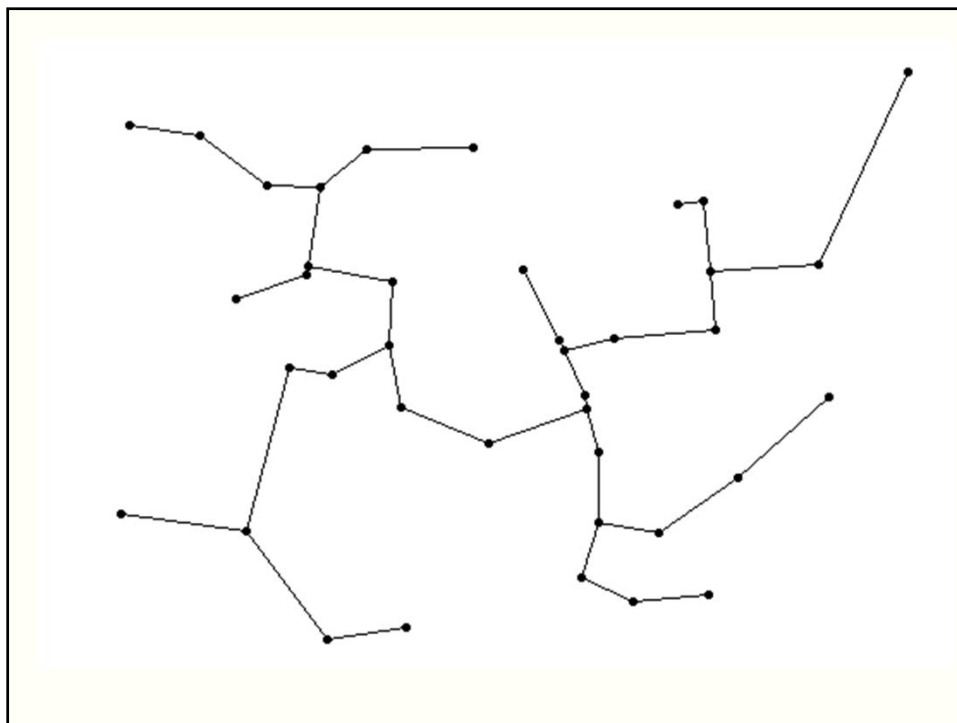
Persistent Homology

Persistent Homology describes the homological features which persist as a single parameter changes

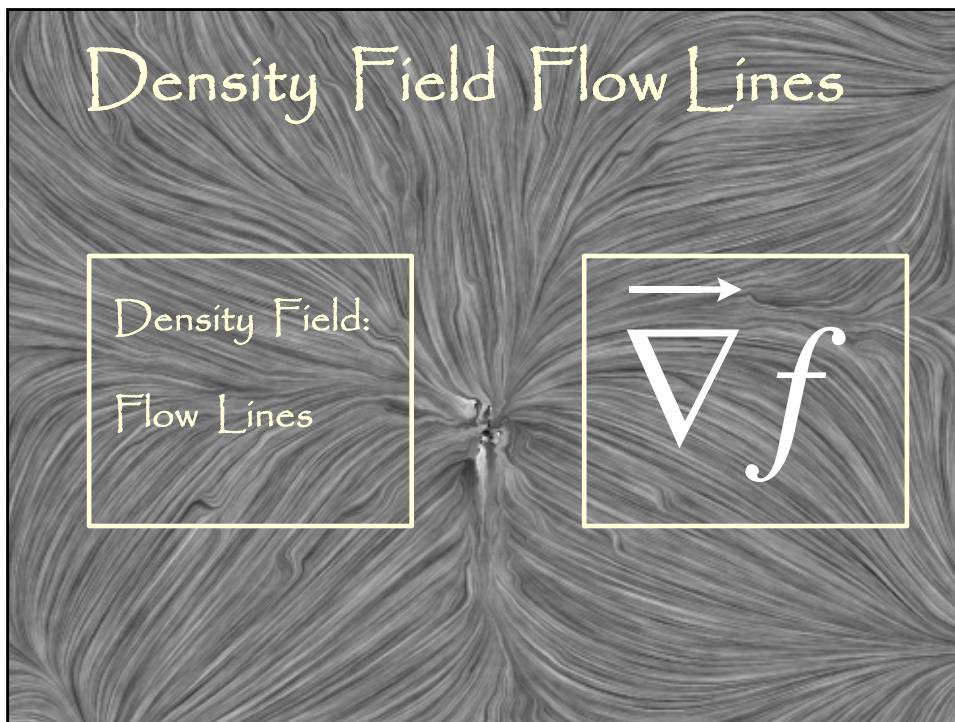
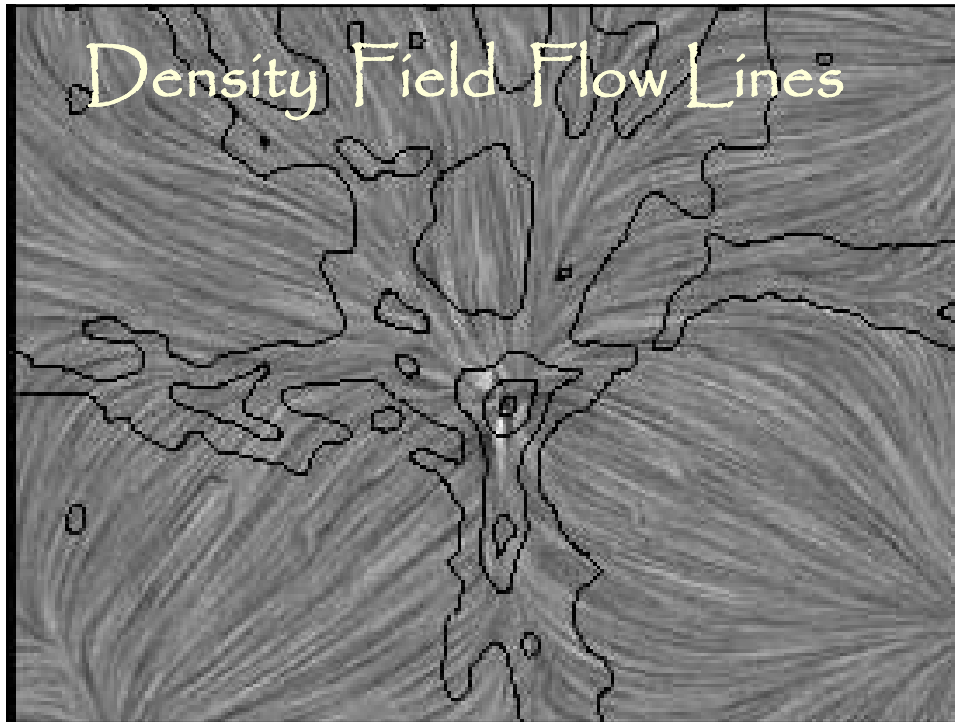




Minimal Spanning Tree



Morse Theory



Density Field Flow Lines

$$\vec{\nabla} f = 0$$

Critical Points:

- Maxima
- Minima
- Saddle Points (of various signature)

Density Field Critical Points:

Ridges:

Connections
Saddle-
Maxima

- Maximum
- ⊠ Saddle
- Minimum

